Aus der Klinik für Neurologie

(Prof. Dr. med. Thorsten R. Döppner, M.Sc.)

der Medizinischen Fakultät der Universität Göttingen

Knockdown of NEAT1 prevents lipid droplet accumulation in microglia after ischemic stroke via autophagy

INAUGURAL-DISSERTATION

zur Erlangung des Doktorgrades

der Medizinischen Fakultät der

Georg-August-Universität zu Göttingen

vorgelegt von

Yongli Pan

aus

Jinan, Shandong, China

Göttingen 2023

Dekan: Prof. Dr. med. W. Brück

Betreuungsausschuss

Betreuer/in: Prof. Dr. med. Thorsten R. Döppner

Ko-Betreuer/in: Prof. Dr. Michael Thumm

Prüfungskommission

Referent/in: Prof. Dr. med. A. Schilling

Ko-Referent/in:

Drittreferent/in:

Datum der mündlichen Prüfung:

Hiermit erkläre ich, die Dissertation mit dem Titel "Knockdown of NEAT1 prevents lipid droplet accumulation in microglia after ischemic stroke via autophagy" eigenständig angefertigt und keine anderen als die von mir angegebenen Quellen und Hilfsmittel verwendet zu haben.

Göttingen, den 12-01-2023

(Unterschrift)

TABLE OF CONTENTS

LIST OF FIGURES

LIST OF TABLES

ABBREVIATIONS

ASO	Antisense oligonucleotide
BBB	Blood brain barrier
BSA	Bovine serum albumin
CNS	Central nervous system
CEs	Cholesteryl esters
DPBS	Dulbecco's phosphate-buffered saline
DMSO	Dimethyl sulfoxide
DNA	Deoxyribonucleic acid
DMEM	Dulbecco's modified Eagle's medium
EDTA	Ethylenediaminetetraacetic acid
EAA	Excitatory amino acids
ER	Endoplasmic reticulum
FBS	Fetal bovine serum
GAPDH	Glycerinaldehyd-3-phosphat-dehydrogenase
HBOT	Hyperbaric oxygen therapy
HIF	Hypoxia-inducible factor
HBSS	Hanks' balanced salt solution
ICH	Intracerebral hemorrhage
IL	Interleukin
IRI	Ischemia-reperfusion injury
LMWHs	Low-molecular-weight heparins
LDs	Lipid droplets
lncRNA	Long noncoding RNA
LDAM	Lipid-droplet-accumulating microglia
miRNA	MicroRNA
MEN	Multiple endocrine neoplasias
mito-mRNAs	mRNAs of nuclear-encoded mitochondrial proteins
Min	Minutes
NEAT1	Nuclear paraspeckle assembly transcript 1
OGD/R	Oxygen glucose deprivation / and reperfusion
PBST	Phosphate-buffered saline-Tween
PLIN2	Perilipin 2
PIC	Protease inhibitor cocktail

PUFAs	Polyunsaturated fatty acids
PPIA	Peptidylprolyl isomerase A
PFA	Platelet activator factor
PDL	Poly-D-lysine
P/S	Penicillin/streptomycin
PVDF	Polyvinylidene fluoride or polyvinylidene difluoride
RIPA	Radioimmunoprecipitation assay
RAPA	Rapamycin
RNA	Ribonucleic acid
ROS	Reactive oxygen species
RT	Room temperature
rt-PA	Recombinant tissue-type plasminogen activator
SDS-PAGE	SDS-polyacrylamide gel electrophoresis
SAH	Subarachnoid hemorrhage
TBST	Tris-buffered saline-Tween
TNF-α	Tumor necrosis factor-alpha
TAGs	Triacylglycerols
UFH	Unfractionated heparin
UK	Urokinase
3-MA	3-methyladenin

ABSTRACT

Lipid droplets (LDs), lipid-storing organelles containing neutral lipids such as glycerolipids and cholesterol, are increasingly accepted as structural markers of inflammation. The nuclear paraspeckle assembly transcript 1 (NEAT1), a long non-coding RNA with over 200 nucleotides, exerts an indispensable impact on regulating autophagy and LDs accumulation in multiple neurological disorders. Interestingly, autophagy can modulate LDs accumulation as well. However, the knowledge about how NEAT1 modulates the formation of LDs in stroke is limited. In this study, primary microglia were isolated and identified from newborn mice. Then an in vitro oxygen-glucose deprivation and reperfusion (OGD/R) model was established, and qRT-PCR and immunofluorescence were employed to identify that NEAT1 and LDs were significantly increased in microglia after exposure to OGD/R. To further explore the mechanism, an antisense oligonucleotide (ASO NEAT1) was adopted to silence NEAT1 in microglia. It was observed that LD formation and autophagy-related protein LC3 were repressed, as exhibited in immunofluorescence and western blot analyses, respectively. Similarly, real-time PCR demonstrated the same observation on LD marker PLIN2, as well as signaling cascades related to autophagy (Atg3, Atg5, Beclin1, and STAT3). Additionally, 3-methyladenin (3-MA) and rapamycin (RAPA) were used to inhibit or activate autophagy, in turn, to illustrate the interaction between autophagy and LD accumulation. RAPA reversed the down-regulated LD accumulation and PLIN2 expression patterns induced by ASO NEAT1 under OGD/R conditions in microglia via immunofluorescence and western blot, whereas 3-MA promoted these effects. This thesis provides insight into NEAT1 knockdown as a potential novel treatment option for stroke by alleviating autophagy and further suppressing LDs.

1. Introduction

1.1. Stroke

Stroke is a major high-risk disease in global public health affecting human health and threatening life worldwide. The disability caused by stroke imposes a huge burden on families and society (Donnan et al. 2008). Every 40 seconds, someone gets a stroke. The disease influences roughly 13.7 million people and causes approximately 5.5 million deaths annually. There are two kinds of stroke, either ischemia or hemorrhage (o. Autor 2019). A hemorrhagic stroke occurs due to the rupture of a blood vessel inside the brain. Ischemic stroke, the main kind of stroke accounting for about 85% of all strokes, is characterized by stenosis or occlusion of an artery, leading to hypoxia and insufficient nutrient supply to the brain, which finally results in neuronal damage. Common signs and symptoms of stroke often include aphasia, hemiparesis, hemispatial neglect, hemianopia, reduced levels of consciousness, headache, and diplopia (Musuka et al. 2015). Statistically, age and gender have a higher risk of experiencing a stroke (Barthels und Das 2020). Treating vascular occlusion usually involves reperfusion and rapid blood flow restoration. Years of research have found that ultra-early intravenous thrombolysis with recombinant tissue-type plasminogen activator (rt-PA) or mechanical thrombectomy via surgery is the most immediate and effective therapy (Balami et al. 2013). However, related studies have shown that the thrombolytic effect of rt-PA in the blood vessel is beneficial but harmful in the brain parenchyma (Zhu et al. 2019). Besides, the rt-PA treatment time window is narrow, with only 4.5 hours (Bai et al. 2019). After treatment, there are many contraindications and a risk of a cerebral hemorrhage. Most patients have different degrees of sequelae due to missing the best time for treatment. Finding an efficient and safe therapy has become an urgent challenge in stroke research.

1.2. Classification and pathophysiology of stroke

According to the pathophysiology of the disease, stroke is divided into two main subtypes: ischemic or hemorrhagic stroke, as previously mentioned. Ischemic stroke is an acute episode of neurological dysfunction triggered by the localized brain, spinal, or retinal ischemia that lasts more than 24 hours (Edlow 2018). In contrast, a transient ischemic attack is "a brief period of neurological impairment caused by focal brain, spinal cord or retinal ischemia that does not result in an acute infarction" (Panuganti et al. 2022). Furthermore, hemorrhagic stroke includes two different types: subarachnoid hemorrhage (SAH) and intracerebral

hemorrhage (ICH) (Krafft et al. 2012). The brain's function and survival depend on continuous oxygen and glucose delivered through the blood. McClendon et al. discovered that even a brief 30-minute maternal hypoxia-ischmia can lead to long-term disturbance of the hippocampus, which is important for learning and memory (McClendon et al. 2019). Ischemia induces a cascade of events leading to dysfunction of two significant injury zones: the infarct core and the penumbra, usually due to thrombosis or embolism in the brain (Zhou et al. 2018). A thrombotic stroke caused by atherosclerosis is most likely caused by vessel constriction. The build-up of fatty plaques will eventually restrict the vascular chamber and create clots, resulting in a thrombotic stroke. An embolic stroke occurs when blood clots or other particles develop elsewhere in the body and move along the circulation to obstruct blood flow to the brain, causing severe stress and irreversible cell death (necrosis) (Kuriakose und Xiao 2020). The infarct area is accompanied by cerebral edema and punctate hemorrhage around the capillaries. Pathological tissues show atrophy in later stages, and necrotic tissue is cleared by phagocytes, leaving scar tissue and cavity (Jordán et al. 2007). The infarct that results from cerebral embolism happens quickly and can produce a red congestive infarct, white color, or mixed ischemia. The brain's nerve cells have the lowest tolerance to ischemia, and 3-4 minutes of focal ischemia already can cause infarction (Hao et al. 2020).

Energy depletion, acidosis, excitotoxicity, an increase in intracellular Ca^{2+}, production of free radicals, apoptosis, disruption of the blood-brain barrier (BBB), and inflammation are the main pathogenic processes of the ischemic cascade (Durukan und Tatlisumak 2007). In the state of ischemia and hypoxia, the energy metabolism of mitochondria changes from aerobic metabolism to anaerobic metabolism, and glucose is metabolized to lactic acid. However, anaerobic fermentation produces much less energy than aerobic oxidation, and its efficiency of ATP production is only 1/18 of the average (Muthaian et al. 2012). Excitatory amino acids (EAA), particularly glutamic acid (Glu), are released and reabsorbed in the central nervous system (CNS) as a result of brain ischemia. So the "excitotoxicity theory" states that the over-activation of EAA receptors in the postsynaptic membrane is a major factor contributing to neuronal damage (Shen Z et al. 2022). According to research by Yang et al., glutamate released by astrocytes during an ischemic stroke modifies synaptic transmission and increases brain injury (Yang J et al. 2019). Moreover, ischemic brain injury is closely linked to an increase in cytosolic Ca^{2+} accumulation as a result of aberrant Ca^{2+} signal transduction. The pathologic studies of cerebral ischemia have found that increased intracellular Ca^{2+} influx in neuronal cells can lead to cell degeneration and death (Kristián 2004). Neuronal degeneration and death caused by excitonic acids and a variety of neurotoxins are always accompanied by cytosolic Ca^{2+} overloaded (Verma et al. 2022). Under normal circumstances, superoxide

dismutase, catalase, peroxidase, and a small number of free radicals exist in the body, which can remove these free radicals without toxic effects on cells (Pham-Huy et al. 2008). When acute cerebral infarction occurs, the common metabolic pathways of neuronal cells are destroyed due to the decrease of oxygen supply and ATP. The aforementioned dynamic equilibrium condition is destroyed, causing a buildup of oxygen-free radicals. The free radicals can act on polyunsaturated fatty acids (PUFAs), induce peroxidation reactions, promote the polymerization and de-polymerization of polysugar molecules, ultimately induce the cross-linking and oxidation of DNA and RNA albumin, resulting in ischemic brain damage (Sun M et al. 2018; Venø et al. 2019). Following brain ischemia, damaged brain cells produce a large number of inflammatory cytokines, including platelet activator factor (PAF), tumor necrosis factor-α (TNF-α), interleukin-1 (IL-1), as well as the expression of adhesion molecules on the surface of endothelial cells, which cross the vascular wall into the brain parenchyma (Anrather und Iadecola 2016; Chamorro et al. 2016; Iadecola et al. 2020).

1.3. Treatment

1.3.1 Thrombolytic therapy

Ultra-early intravenous thrombolytic therapy is the preferred option for treating an acute cerebral infarction. The thrombolytic drugs rt-PA and urokinase (UK) are routinely utilized (Sun F et al. 2020). Rt-PA is a particular thrombolytic agent that is safe and effective in treating ultra-early cerebral infarction with a time window of 4.5 hours (Prabhakaran et al. 2015). It not only has a high affinity for fibrinogen in thrombus but also has a high affinity and specificity for fibrinogen-bound fibrin. When the latter is degraded into the lysozyme of blood fibrin, the thrombus is dissolved (Bhaskar et al. 2018). It remains the primary therapy for the majority of stroke patients and does not increase the incidence of a cerebral hemorrhage. Hong et al. consistently used the metric routinely to quantify the effectiveness of thrombolytic treatment for cerebral infarction patients within 3 hours after onset and found it could add the equivalent of 4.4 years of wellness without impairment (Hong und Saver 2010). Although reperfusion is essential to restore ischemic brain function, paradoxically, it can also cause secondary brain injury, termed ischemia-reperfusion injury (IRI). The main reason causing the pathological reaction of IRI is the brain damage due to oxidative stress produced by hypoxia and glucose deprivation. Other processes that are compromised involve mitochondrial metabolism, resynthesis of pro- and anti-apoptotic proteins, and neuronal response (Wu M et al. 2021). The present techniques of therapy mainly focus on pharmacological and mechanical thrombolysis, although the clinical efficacy

is limited.

1.3.2 Anticoagulant therapy

Anticoagulant therapy is a standard treatment for the prevention and treatment of thrombosis. Direct oral anticoagulants and heparin are commonly used in clinical therapy (Chaves und Caplan 2000). Low-molecular-weight heparins (LMWHs) are a novel form of anticoagulants created from unfractionated heparin (UFH), which has a longer half-life, higher bioavailability, less adverse reactions, and does not need laboratory monitoring (Sandercock und Leong 2017). Experimental work has shown that LMWHs are the most suitable inhibitors of active coagulation factor Xa (FXa) and thrombin, which effectively inhibit thrombosis without affecting the coagulation function and reduce bleeding and other complications (Sandercock et al. 2008). Effective anticoagulant therapy can reduce the severity of a stroke and improve the survival rate. In stroke patients, anticoagulant therapy based on low-dose UFH combined with LMWHs can enhance coagulation function, reduce thrombotic complications, promote neurological function restoration, and improve overall survival (Kiphuth et al. 2009).

1.3.3 Antiplatelet aggregation therapy

Platelet activation is essential for clotting and normal hemostasis through maintaining the integrity of blood vessels. Theoretically, patients' platelet function under pathologic conditions is often hyperactive, resulting in occlusive thrombus formation and stroke (Yeung et al. 2018). Therefore, antiplatelet therapy (mainly aspirin and P2Y12 receptor antagonists) is widely used to inhibit platelet aggregation in clinical practice, which achieves an anticoagulation effect and restores spontaneous circulation (Chong und Mohr 2005). Aspirin is a cyclo-oxygenase inhibitor and the most commonly used antiplatelet drug in clinical practice. Judge et al. performed a study among 83,749 participants and confirmed that aspirin lowers stroke risk in pregnant women with pre-existing hypertension (Miller et al. 2019). In patients with acute cerebral infarction, aspirin was effective in doses of 100-300mg/d within 48 hours of onset and could significantly reduce the recurrence rate and mortality (Sandercock et al. 2014). Ozagrel is another new antiplatelet drug that effectively impedes the generation of thromboxane A2 (TAX2) synthase. It can inhibit platelet aggregation, promote prostacyclin production to expand cerebral blood vessels, inhibit cerebral vasospasm, and effectively increase cerebral blood flow to the brain (Bhatia et al. 2021). A randomized controlled trial by Zhang et al. demonstrated that ozagrel improves the

neurological impairment of acute ischemic stroke patients (Zhang J et al. 2012).

1.3.4 Neuronal protection

Ordinarily, the metabolic rate of mammals is ultimately associated with maintaining body temperature. Mild hypothermia therapy is defined as a body core temperature below 35 °C, also known as hibernation therapy or artificial hibernation therapy (Forreider et al. 2017). Mild hypothermia therapy can reduce free radical generation and excitatory amino acid release, further reducing the permeability of the BBB and brain metabolic rate, therefore having a neuroprotective effect on ischemic cerebrovascular disease (Drew et al. 2001). Hyperbaric oxygen therapy (HBOT) is a well-known non-invasive treatment method using almost pure oxygen to speed up the healing of carbon monoxide poisoning in recent years (Ortega et al. 2021). Numerous early trials have shown that HBOT has protective benefits in several stroke animal models, including better neurobehavioral outcomes, alleviated brain lesion volume, and reduced BBB damage (Veltkamp et al. 2000; Veltkamp et al. 2005; Veltkamp et al. 2006). It can significantly improve the dissolved oxygenation level at the area of focal ischemia, reduce early tissue acidosis, regulate cerebrovascular flow, and promote the formation of collateral circulation, thereby reducing brain edema and intracranial pressure. Additionally, it can effectively lower the synthesis of hypoxia-inducible factor-1 (HIF-1) and its downstream target factors to limit neuronal cell death from promoting the regeneration and remodeling of neuronal cells (Bennett et al. 2005; Thiankhaw et al. 2021). Besides hypothermia and HBOT therapy, multiple drugs for the treatment of strokes are available, such as cytidine-5'-diphosphocholine, neuropeptides, neurotrophic factors, and ergotoxine (Adibhatla und Hatcher 2005; Harada et al. 2012; Mattson 2008).

1.3.5 Stem cell therapy

Stem cells are distinguished from other kinds of cells since they are available to renew themselves and are proficient in differentiation into multiple cell types. Decades of experimental evidence have pointed to the therapeutic possibility of stem cell-based treatment to enhance recovery from stroke, even though much still needs to be elucidated (Kwak K et al. 2018). It has been demonstrated that stem cells may regulate immune cell activity and pro- or anti-inflammatory signals to systemically suppress over-responsive immune reactions (Jia et al. 2022). Another primary mechanism of stem cell therapy following stroke is promoting vascular remodeling and neurogenesis (Taguchi et al. 2004). Several different routes of stem cell administration in stroke have been investigated, and all

showed therapeutic efficacy (Chrostek et al. 2019; Yarygin et al. 2021). However, stem cell-based treatment is still in its early stages of clinical use. While allogeneic cells have been used in most recent clinical trials, the possibility of allergic reaction remains (Kawabori et al. 2020). Additionally, the cell viability and migration of transplanted stem cells into lesion sites should be improved (Kwak KA et al. 2018).

1.4. LncRNAs in stroke

Long noncoding RNAs (lncRNAs) are a kind of ribonucleic acid (RNA) with a length of more than 200 nucleotides but no capacity to code for proteins (Karlsson und Baccarelli 2016). Numerous studies have previously shown that lncRNAs have a wide range of impacts on various biological processes, such as biogenesis, transcription, translation, splicing, and stabilization (Tao et al. 2019). In cells, lncRNAs can modulate chromatin function by interacting with proteins, deoxyribonucleic acid (DNA), and RNA (Statello et al. 2021). In general, lncRNAs predominantly are located inside the nucleus, whereas certain lncRNAs preferentially reside in the cytoplasm of cells (Ji et al. 2015). It was shown that cytoplasmic lncRNAs can promote or block translation by binding to mRNAs or act as endogenous sponges of microRNA (miR) to inhibit their downstream target genes (Lanzillotti et al. 2021). LncRNAs in the nucleus recruit chromatin modification complexes to regulate the chromatin state and then regulate the expression of adjacent or distant genes (Gao et al. 2020; Juni et al. 2022). The significance of lncRNAs in the formation and maintenance of CNS homeostasis is abundantly expressed. At the same time, considerable experiments show that ischemic stroke aberrantly changes the expression profile of lncRNAs (Wang S et al. 2018). Following ischemic stroke, abundant evidence has proclaimed that lncRNAs participate in the complex molecular process of ischemic cascade and influence the ischemic injury progression through calcium overload, glutamate toxicity, oxidative stress, inflammatory response, vascular injury, neuronal necrosis, neuroprotection, synaptic function (Bao et al. 2018; Ghafouri-Fard et al. 2020; Wang Q et al. 2022). Some abnormally expressed lncRNAs have been found in both ischemic stroke patients and animal models of this disease. Among these, NEAT1 was identified, making it a viable target for ischemic stroke treatment (Jin F et al. 2021; Li P et al. 2020).

1.5. NEAT1

NEAT1 is an unspliced, polyadenylated lncRNA produced by RNA polymerase II from a

region on human chromosome 11q13 known as multiple endocrine neoplasias (MEN) type I, which yields two unique isoforms through separate RNA regulatory processes, NEAT1-1 (3.7 kb) and NEAT1-2 (23 kb) (Vlachogiannis et al. 2021). NEAT1-1 is widely represented in the majority of organs and tissues in the adult mouse, especially in the stomach, lung, kidney, and heart, but with relatively low expression in the brain. NEAT1-2, on the other hand, is found in just a fraction of cells in the gastrointestinal tract (Nakagawa et al. 2011). NEAT1 is enriched in the nucleus and serves as a crucial structural framework for paraspeckle protein assembly, enabling paraspeckle proteins to form organized structures, such as PSPC1, P54NRB/NONO, and SFPQ/PSF (Bu et al. 2020). Due to its indissociable structural scaffold of paraspeckles, NEAT1 may be essential in some applications. Imamura et al. discovered that the stimulus-responsive cooperative interaction between NEAT1 and SFPQ stimulates transcriptional stimulation of antiviral genes, including factors like interleukin-8 (IL-8) (Imamura et al. 2014). The loss of mitochondrial proteins is also known to influence NEAT1 expression, and NEAT1 depletion has substantial consequences on mitochondrial dynamics and functions by changing the sequestration of mRNAs of nuclear-encoded mitochondrial proteins (mito-mRNAs) in paraspeckles (Wang Y et al. 2018). Furthermore, NEAT1 acts as a ceRNA to interact with mRNA, miR, or DNA to alter the expression of subsequent proteins (Zhang J et al. 2021).

Numerous studies have shown an intensive upregulation of NEAT1 in various malignancies, like breast cancer (Ke et al. 2016; Li et al. 2017), respiratory cancer (Jen et al. 2017; Wu F et al. 2019), hepatocellular carcinoma (Fang et al. 2017; Wang et al. 2017), ovarian cancer (An et al. 2017; Liu Y et al. 2018), and colorectal cancer (Liu H et al. 2020; Zhong et al. 2018), indicating a lower chance of survival. Concerning non-cancerous diseases, NEAT1 was revealed to be involved in immunological reactions in the brains of mice infected with the Japanese encephalitis virus (Kung et al. 2013). NEAT1 dysregulation has been documented in individuals with asthma, systemic lupus erythematosus, arthritis, inflammatory bowel disorder, and sepsis. For instance, Li et al. studied 170 patients and discovered that the asthma group had higher NEAT1 expression than the healthy controls (Li Y et al. 2020). NEAT1 has been reported adversely associated with miR-21 and miR-125a in allergic rhinitis (Wang R et al. 2021). Additionally, silencing NEAT1 boosted the expression of miR-129 and miR-204 to reduce the fibroblast-like synoviocytes cells' proliferation and inflammatory cytokines production in allergic rhinitis by the MAPK/ERK pathway (Chen J et al. 2021). Meanwhile, NEAT1 promotes the activation of several inflammasomes and enhances cytokine production (Zhang P et al. 2019). Furthermore, NEAT1 is also engaged in the pathogenesis of lupus (Zhang F et al. 2016). Experiments in disease models in vitro and in

vivo have verified some biological functions in the development and progression of neurodegenerative disorders, such as Huntington's disease, multiple sclerosis, Alzheimer's disease, Parkinson's disease, and amyotrophic lateral sclerosis (Prinz et al. 2019). Santoro et al. investigated an increase of NEAT1 in the serum of patients with multiple sclerosis by screening 84 lncRNAs (Santoro et al. 2016). Another publicly available microarray data analysis of 151 Parkinson's disease patients and 130 control subjects also reported a 1.5 times upregulation of NEAT1 in Parkinson's disease patients (Mariani et al. 2016).

1.6. Post-stroke lipid droplet

Lipid droplets (LDs), also known as lipid bodies, oil bodies, fat bodies, or adiposomes, were initially discovered under light microscopy as cellular organelles in the nineteenth century (Greenberg et al. 1991). LDs are made up of a hydrophobic core of neutral lipids, mainly triacylglycerols (TAGs) and cholesteryl esters (CEs), enclosed by a phospholipid monolayer equipped with various proteins that govern LDs activity (Olzmann und Carvalho 2019). These LDs store metabolic energy to act as lipid reservoirs to provide substrates for membrane formation and energy metabolism for cells (Walther und Farese 2012). Almost all cells can form and store LDs. Exogenous lipid uptake stimulates the accumulation of LDs, which can be observed in enterocytes with rapid production of cytosolic LDs in mice exposed to a high-fat diet (Soayfane et al. 2016). Intriguingly, LDs also form in response to nutrient deprivation (Hariri et al. 2018; Kwon et al. 2017). Besides nutrient status, mitochondrial dysfunction, ER stress, hypoxia, inflammation, and oxidative stress all impact LDs formation (Ralhan et al. 2021). Biogenesis of LDs sprouts from the endoplasmic reticulum (ER) through a cascade of biochemical events and converting fatty acids or cholesterol into ultimate neutral lipid products, TAGs and CEs, respectively. Alternatively, a nascent LD may further grow and expand via LDs fusion, resulting in TAGs incorporation (Dhiman et al. 2020). Biological research about LDs in the brain has been steadily growing in recent years. Lipids account for more than half of the dry weight of human brain (Yu et al. 2020). Even though not widely employed to provide energy to the brain, lipids metabolism is closely related to maintaining normal brain homeostasis and neuronal and neuroglial cell function. Lipidomic profiles have already described differences across various cell types in the brain. Consistently, the relative number of LDs fluctuates within various brain cells (Fitzner et al. 2020). LDs are expressed at low levels under normal brain physiology, whereas accumulating evidence suggests an aggregation in the brain during development, aging, and pathological state, such as neurodegenerative diseases (Parkinson's disease, Huntington's

disease, Alzheimer's disease), and cancer, particularly in neuroglial cells (astrocytes and microglia).

Microglia are the most common macrophage-like resident glial cells in the CNS to respond against infections, antigen presentation, and the intrinsic inflammatory response. Microglia can directly interact with neurons, astrocytes, endothelial cells, oligodendrocytes, or other multitudinous cell types to eliminate dead cells, microbes, protein aggregates, and soluble antigens, which are dangerous for the CNS (Colonna und Butovsky 2017). Microglia retain a ramified phenotype under physiological conditions with a small soma and processes actively surveying their local environment to mediate brain homeostasis. Following a stroke, microglia immediately are activated, migrate to the affected region, stimulate downstream cell signaling cascades to the injured area and secret some immunomodulatory molecules, such as cytokines, chemokines, and free radicals, which is then followed by invasion of other immune cells (Woodburn et al. 2021). The accumulation of LDs in microglia in the aging brain and various neurodegenerative disease mouse models has been recently recognized as "lipid-droplet-accumulating microglia" (LDAM) (Marschallinger J. et al. 2020). LDAM revealed microglial dysfunction, such as phagocytosis deficits, excessive production of proinflammatory cytokines, increased generation of reactive oxygen species (ROS), and decreased cholesterol export compared with neuroprotective LPS-activated LD-rich microglia (Marschallinger J et al. 2020). Gai et al. have shown that lipids accumulate in synuclein-containing Lewy bodies purified from human Parkinson's disease brains (Gai et al. 2000). The discovery from Cole et al. raises the possibility that synuclein aggregation's initial phases occur on membrane surfaces rather than in the cytosol (Cole et al. 2002). In the past few years, there has been a growing number of studies and evolving knowledge regarding the involvement of LDs in neurodegenerative diseases. However, there is only little knowledge about the formation of LDs after cerebral infarction up to now. Only one article published in 2001 illustrated magnetic resonance lipid signals in stoke rat brains correlated with neutral lipid accumulation (Gasparovic et al. 2001).

1.7. Post-stroke autophagy

Autophagy is essential for cell homeostasis and energy metabolism. Firstly, when hypoxia, infection, oxidative stress, nutrient deficiency, and other adverse factors occur, cells can initiate autophagy to respond. The degradation products, such as free fatty acids, nucleotides, and amino acids, can be recycled (He et al. 2018). Secondly, as a self-stabilizing housekeeping mechanism, autophagy can regulate the metabolism of the endoplasmic reticulum,

peroxisomes, and mitochondria in cells (Rabinowitz und White 2010). In addition, as a defense mechanism, autophagy can remove damaged metabolites and organelles in cells, reorganize at the subcellular level, and maintain the stability of the internal environment (Green und Levine 2014). Under physiological or pathological conditions, double-layer membrane package proteins or organelles from the ER and Golgi apparatus form autophagosomes, then combine with lysosomes to form autophagy-lysosome to make many kinds of enzyme digestion and degradation (Zhang Z et al. 2021). The decomposed amino acids, nucleotides, and free fatty acids can be reused by cells to meet metabolic needs and achieve the renewal of some organelles. Under normal circumstances, autophagy maintains a very low baseline in order to eliminate and degrade the damaged, aging, and transgender biological macromolecules, such as protein and nucleic acid (Ryter et al. 2013). Therefore it provides the raw material for the reconstruction, regeneration, and repair of cells, meets the needs of the metabolism, and achieves cell recycling (Mizushima und Komatsu 2011). Under the stimulation of exogenous factors, including nutrition deficiency, hunger, growth factors, hypoxia, infection, and high energy demand, autophagy can adapt to remove useless and energy-consuming senescent organelles with misfolded proteins, degrade them and generate energy for cell utilization. When cerebral IRI occurs, autophagy-related signaling pathways are dramatically stimulated (Wang P et al. 2018). In recent years, ischemia-reperfusion cell culture and animal models have confirmed that autophagy, moderately active under hunger, hypoxia, and other cases, not only contributes to the protection of poor nutrition cells but also can promote their survival (Green und Levine 2014). Carloni et al. established a neonatal rat model of ischemic brain damage, detected the expression of Beclin1 and cell apoptosis by western blot and immunohistochemistry, and discovered that Beclin1 expression was up-regulated in the cortex and hippocampus of rats 4 hours after hypoxia, along with a reduced number of necrotic nerve cells. They confirmed that the protective effect of autophagy in brain injury was driven by ischemia and oxygen deprivation (Carloni et al. 2008). However, if autophagy is overactivated, it can cause cell lysis and promote cell death, namely autophagic cell death, which is often accompanied by apoptosis and necrosis. When autophagy is over-activated, it may trigger the cells' apoptosis program and cause neuronal death.

Current studies believe two main molecular regulatory pathways are involved in autophagy: the mTOR-dependent and the mTOR-independent pathway (Sarkar 2013). Within the dependent pathway, mTOR, a component of the PI-kinase-related kinase family, is critical for autophagy (Jung et al. 2010). The expression of cell receptors is enhanced by stimulation of insulin and growth factors, the corresponding target molecules are activated with the

assistance of ligands, and finally, the phosphorylation of PIP2 is promoted (Hung et al. 2012). TSC1/2 protein, located downstream of the ClassI PI3K/PKB pathway, can inhibit mTOR function and initiate autophagy. However, TSC2 is inactivated when it is phosphorylated by AKT, which further activates Rheb, promotes the activation of the mTOR complex, and finally antagonizes autophagy inversely (Huang und Manning 2008). So far, mTOR-related inhibitors include rapamycin (RAPA) and related derivative RADO01. In addition, related molecular pathways independent of mTOR include Gai3, class III PI3K complex (Klionsky und Emr 2000; Martin et al. 2014).

As mentioned before, microglia are the most abundant resident glial cells in the CNS and play a crucial role in regulating neurological functions. Microglia cells were shown to undergo the autophagy process in a chronic cerebral hypoperfusion model in mice caused by permanent stenosis of the bilateral common carotid artery (Yang Z et al. 2014). The overactivation of autophagy in microglia induced by sphingosine kinase 1/sphingosine-1-phosphate (SphK1/S1P) seems to be related to the exacerbation of neuronal injury following ischemia/reperfusion (Zeng et al. 2022). Activation of autophagy by microglia takes place via a range of signaling pathways involved in ischemic stroke, such as PI3K/Akt-mTOR, AMP/AMPK-mTOR, HIF-1 α /BNIP3, and ER stress-autophagy axis (Qin et al. 2022). Appropriate activation of autophagy can reduce microglial activation and promote microglia phenotype polarization to inhibit inflammasome activity (Peng et al. 2022). As a result, it reduces neuroinflammation caused by cerebral ischemia, eventually acting as a neuroprotectant and improving the stroke outcome. In comparison, excessive autophagy results in cell death and exacerbates brain ischemia injuries.

1.8. The purpose of this thesis

LDs, lipid-storing organelles containing neutral lipids like glycerolipids and cholesterol, are gaining importance as structural indicators of inflammation and lipid accumulation in multiple disorders. NEAT1, a long non-coding RNA with over 200 nucleotides, exerts indispensable impacts on regulating autophagy. Interestingly, autophagy can modulate LD accumulation as well. Recently, it was shown that LDs accumulate in microglia in the aging brain, as well as in some neurodegenerative disease mouse models. Meanwhile, transcriptome-wide analysis has proven that NEAT1 has an inflammatory function in experimental ischemic stroke. Intriguingly, the blockade of NEAT1 represses lipid uptake in human macrophages' THP-1 cells. Despite this findings, in the knowledge regarding the interplay of LDs, stroke and NEAT1 is still scarce. Therefore, the present study hypothesizes

that the knockdown of NEAT1 prevents from LD accumulation in primary microglia via the autophagy pathway under stroke condition.

2. Materials and Methods

2.1. Lab equipment

Table 1: Lab equipment

Device	Model	Company
Centrifuge	Microcentrifuge 5415 R	Eppendorf, Germany
Freezer (-20 °C)	LGex3410	Liebherr, Switzerland
Freezer (-80 °C)	Heraeus	Fisher Scientific GmbH, Germany
Refrigerator +4 °C	471-1076	Liebherr, Switzerland
Ice machine	ZBE 70-35	Ice Systems, UK
Nanodrop One	ND1000 spectrophotometer	Fisher NanoDrop, USA
Sartorius™ arium pro VF Ultrapure Water System	Kurzanleitung arium® 611	Sartorius AG, Germany
Microplate Reader	Tecan Sunrise	Tecan Group AG, Switzerland
Western Blotchamber	Mini Protean® Tetra Cell	Bio-Rad, USA
Workbench	Thermo Scientific™ Heraguard™ Clean air workbench	Fisher Scientific GmbH, Germany
Incubator	Thermo Scientific™ Heracell™ 150i CO_2-incubator	Fisher Scientific GmbH, Germany
Microscope	Zeiss Axiovert 25 inverse microscope	Leica, Germany
Microscope	Zeiss Stemi 2000 ZOOM stereomicroscope	Leica, Germany
Water bath	WNB45	Memmert GmbH + Co. KG, Germany

Vortexer	RS-VA10	Phoenix Instrument, Germany
LightCycler	480 II 28572	Roche Diagnostics GmbH, Germany
Western Blottransfer system	Trans-Blot Turbo Transfer System	Bio-Rad, USA
ECL machine	Chemidoc Station	Biorad, USA
Shaker	IKA-VOBRAX-VXR	IKA®-Werke GmbH & Co. KG, Germany

2.2. Buffers and Solutions

Table 2: Buffers and solutions

Buffer and solutions	Composition
Western Blottransfer buffer (10x pH 8.3)	30.25 g Tris (25mM) 144 g Glycine (192mM) 1000 ml ddH2O
Protein Electrophoresis buffer	15.12 g Tris (250mM) 71.25 g Glycine (1.9 M) 5 g 1% SDS 500 ml ddH2O
Western Blottransfer buffer (10x pH 8.3)	30.25 g Tris (25mM) 144 g Glycine (192mM) 1000 ml ddH2O
BSS0 10x stock solution	800 ml ddH2O 68 g NaCl 4 g KCl 2 g $MgSO_4$ 1.4 g $NaH_2PO_4 \bullet H_2O$ 431 ml ddH2O
BSS0 1x solution	50 ml 10x BSS0 13.1 ml 1 M NaHCO3 5 ml 1 M HEPES

RIPA buffer	166µl 30 mM Glycine 900µl 1 M CaCl2 25 mM Tris-HCl pH 7.6 150 mM NaCl 1% NP-40 1% Sodium deoxycholate 0.1 % SDS
SH-SY5Y culture medium	450ml DMEM (4.5 g/L Glucose, stable Glutamine) 50ml FBS 5ml Penicillin-Streptomycin 5ml GlutaMAX™-I (100x)
Microglia culture medium	450 ml DMEM/F12 (1:1, stable Glutamine) 50ml FBS 5ml Penicillin-Streptomycin

2.3. Chemicals and Materials

Table 3: Chemicals

Chemical	Number	Manufacturer
Dimethyl sulfoxide	2380.1000	CHEMSOLUTE®, Germany
0.5% Trypsin-EDTA (10x)	15400-054	Fisher Scientific GmbH, Germany
Ethanol	2236.1000	CHEMSOLUTE®, Germany
Boric acid	B-9645	Sigma-Aldrich Chemie GmbH, Germany
DMEM (4.5 g/l glucose)	P04-04500	PAN-Biotech, Germany
Isopropanol	9866.5	Carl Roth GmbH + Co. KG, Germany
RIPA Lysis and Extraction Buffer	89900	Thermo Fisher Scientific, USA

Clarity Western ECL Substrate	1705061	Bio-Rad Laboratories GmbH, Germany
Methanol	8.22283.2500	Sigma-Aldrich Chemie GmbH, Germany
Glycine	G8898	Sigma-Aldrich Chemie GmbH, Germany
Tris	1.08382.1000	Sigma-Aldrich Chemie GmbH, Germany
DNase I Amplification Grade Kit	AMPD1-KT	Sigma-Aldrich Chemie GmbH, Germany
Dulbecco's Phosphate Buffered Saline	D8537-500ML	Sigma-Aldrich Chemie GmbH, Germany
FBS Superior	S06510	Sigma-Aldrich Chemie GmbH, Germany
GlutaMAX™-I (100x)	35050-061	Fisher Scientific GmbH, Germany
Triton X-100	T8787	Sigma-Aldrich Chemie GmbH, Germany
Powdered milk	1.15363.0500	Sigma-Aldrich Chemie GmbH, Germany
LightCycler® 480 SYBR Green I Master	04887352001	Roche Diagnostics GmbH, Germany
Penicillin-Streptomycin	15140-122	Fisher Scientific GmbH, Germany
Rapamycin	HY-10219	MesChemExpress, Germany
Revert Aid H Minus First Strand cDNA Synthesis Kit	K1632	Fisher Scientific GmbH, Germany
Trypan Blue Solution 0.4%	15250-061	Fisher Scientific GmbH, Germany

BCA Protein Assay Kit	23225	Thermo Fisher Scientific, USA
ASO NEAT1	Customized	Integrated DNA Technologies, Germany
ASO Scramble	Customized	Integrated DNA Technologies, Germany
Turbofect	R0534	Thermo Fisher Scientific, USA
TRIzol Reagent	15596026	Fisher Scientific GmbH, Germany
Chloroform	7554.1	Carl Roth GmbH + Co. KG, Germany
3-MA	M9281	Sigma-Aldrich Chemie GmbH, Germany

Table 4: Materials

Consumable	Provider Information
6-well plates	Sarstedt, Nümbrecht, Germany
24-well plates	Sarstedt, Nümbrecht, Germany
96-well plates	Sarstedt, Nümbrecht, Germany
Bottle-Top-Filter with SFCA membrane, ∅ 75 mm, pore size 0.2 µm, 500 ml	Carl Roth GmbH + Co. KG, Karlsruhe, Germany
Cell culture flasks w/ ventilation cap for adherent cells (25cm^2, 75 cm^2)	Sarstedt, Nümbrecht, Germany
Centrifugation tubes (15 ml)	Sarstedt, Nümbrecht, Germany
Centrifugation tubes (50 ml)	Sarstedt, Nümbrecht, Germany
Glass Pasteur pipettes (150 mm, 230 mm)	Th. Geyer Ingredients GmbH & Co. KG, Renningen, Germany

Pipette tips w/ filters, sterile (10 µl, 100 µl, 1000 µl)	Starlab, Hamburg, Germany
Pipette tips w/o filters (200 µl, 1000 µl, 5000 µl)	Sarstedt, Nümbrecht, Germany
Reaction tubes (1.5 ml, 2.0 ml)	Sarstedt, Nümbrecht, Germany
Serological pipettes (2 ml, 5 ml, 10 ml, 25 ml, 50 ml)	Sarstedt, Nümbrecht, Germany
Parafilm	Bemis NA, Neenah, USA
Mr. Frosty Freezing Container	Thermo Fisher, USA
Syringe 10 ml	BD, USA
CryoPure Tube 1.0 ml	Sarstedt, Germany
Cell Scraper	CytoOne, USA
Gloves	TH.GEYER, Germany
96 well plate for PCR	Biozym, USA
0.2 ml tube for PCR	Biozym, USA
Microseal 'B' seal Seals for PCR	BIO-RAD, Germany

2.4. Software

Table 5: Software for data analysis

Software	Manufacturer
Microsoft PowerPoint 2016	Microsoft, USA
Microsoft Word 2016	Microsoft, USA
Microsoft Excel 2016	Microsoft, USA
GraphPad Prism 9	GraphPad Software, USA
Image lab	Bio-Rad, USA
Image J	LOCI, USA

2.5. Isolation and culture of primary microglia cells

Primary microglia were isolated using the traditional enzyme digestion approach with slight modification (Lian H et al. 2016). In brief, the isolation can be divided into two parts: the mixed glial cell culture and the isolation and purification of primary microglia. The dissection tools and workplace were sterilized with 75% ethanol. Microglia were generated from cerebral cortices and hippocampi of newborn (P0) WT C57BL/6J mice and cultivated in complete Dulbecco's modified Eagle's medium (DMEM), added with 10% fetal bovine serum (FBS) and 1% penicillin/streptomycin (P/S). Pups were decapitated, and the head was placed in a 6 cm Petri dish containing 5 ml of pre-cooled Hanks' balanced salt solution (HBSS). Next, the scalp was cut open. Pointed tip forceps were used beneath the skull but above the brain tissue to remove the skull and the brain can be easily scooped out. Then the brain was transferred into a new dish with 2 ml cold HBSS under a dissection microscope. With a sterile blade, both the cerebellum and the olfactory bulbs were dissected from each brain. Meninges were separated and then the cortices and hippocampi were isolated with forceps. Afterward, these cortices and hippocampi were transferred to a 15 ml falcon tube with 1 ml 0.25% trypsin and digested for 15 min at 37 °C in a water bath. After 15 min, 200 µl of 10 mg/ml DNase was added to break down the sticky DNA produced by dead cells. Then the cell suspension was centrifuged at 300 x g for 5 min at room temperature (RT). The pellet was gently resuspended in 5 ml warm culture medium with a 1 ml pipet tip before being transferred to a 15 ml tube to be centrifuged at 300 x g for 5 min. After centrifugation, the cells were collected and then resuspended in 15 ml of complete astrocyte medium (DMEM supplemented with 10% FBS and 1% P/S) before being grown in poly-D-lysine (PDL)-coated T75 flasks in an incubator at 37 °C with 5% CO_2. The culture medium was changed the next day to eliminate the cell debris, and every five days afterwards. After 5−7 days, astrocytes established an adherent cellular layer at the bottom of the flask, with microglia growing on top of it. Finally, seed the cells at 50000 cells/cm^2 in plates or staining slides for the subsequent experiments, in which cells were grown with DMEM/F12 containing 10% FBS and 1% P/S.

2.6. Establishment of OGD model

The oxygen-glucose deprivation (OGD) model was established to create ischemic conditions in vitro. Primary microglia were exposed to OGD when they achieved 80% - 90% confluency and were washed twice using Dulbecco's phosphate-buffered saline (DPBS), cultivated in a

glucose-free balanced salt solution (BSS0), and subsequently transported to a hypoxic incubator with 95% N_2 / 5% CO_2, and 70% humidity at 37 °C. After the respective incubation time, the cells were moved from the chamber, and the BSS0 was replaced with either DMEM/F12 cell culture medium or other media with additional factors. After that, the cells were employed for further analysis, including cell viability testing, RNA isolation, protein collection, and staining.

2.7. Transfection

The cells were cultured according to the standard requirements. After trypsinization, the isolated and purified microglia were spread to six-well plates, achieving a cell final confluency of 80 to 90% at the time of transfection with 2'-OMe antisense oligonucleotides (ASO). ASO NEAT1 (5'-GGAAATCATAGAGGACAGGC-3') or ASO Scramble (5'-GAAGAAGTACGAAGTGACGC-3') were synthesized by the INTEGRATED DNA TECHNOLOGIES company (San Diego, USA). Cells were transfected with turbofect (Fisher Scientific GmbH, Germany) and divided into three groups: (1) Blank control group, only added turbofect reagent; (2) Negative control group, transfection with ASO Scramble; (3) Knockdown group, transfection with ASO NEAT1. Different concentrations of 100 μM ASO NEAT1 and corresponding ASO Scramble were diluted with serum-free DMEM/F12 without antibiotics to find the highest efficiency to knock down NEAT1. The transfection reagent (turbofect) was briefly vortexed, added to the diluted ASO NEAT1 and ASO Scramble at the ratio of 1:2, and mixed thoroughly, then left for 20 min at RT. Finally, mixed ASO NEAT1 and ASO Scramble were added to the cell culture plates before returning the cells to the incubator. Within one day, cells were replaced with a new solution containing FBS and antibiotics for subsequent experiment. The levels of NEAT1 and protein expression following ASO transfection were determined using real-time PCR and western blot, respectively.

2.8. Cell viability assay

The cells were seeded at a density of 20,000 in a 24-well plate. The growth of cells was observed after 48 hours of culture. After OGD treatment, 100 μl of 5 mg/ml 3-(4,5-dimethylthiazol-2-yl)-2,5-diphenyltetrazolium bromide (MTT) was given to each well (containing 1ml of medium) of each group to achieve approximately a working concentration of 0.5 mg/mL MTT. Then the 24-well plates were placed at 37 °C and incubated for 3 hours

in a standard incubator containing 5% CO_2. Subsequent observation under a light microscope revealed the formation of black formazan crystals in the cell culture plates. By shaking for 3 to 5 min at RT, the reaction was stopped after replacing the MTT solution with 1 ml of dimethyl sulfoxide (DMSO) to solubilize and dissolve the formazan crystals. Finally, the supernatant was transferred to a 96-well plate and a microplate reader was utilized to determine its absorbance at 565 nm.

2.9. RNA extraction and quantitative real-time PCR analysis

2.9.1 Total RNA extraction

Total RNA was isolated using TRIzol as directed by the manufacturer's instructions (Fisher Scientific GmbH, Germany). In brief, the medium was removed from the well and the cells were washed twice with 1x DPBS. Afterward, the DPBS was discarded, and 500 µl TRIzol reagent was applied to each well of 6-well plates. The cells were scraped off the plate and two wells of the TRIzol/cell lysate were transferred into a sterile 1.5 mL Eppendorf reaction tube and left at RT for 10 min. Subsequently, each tube was added with 200 µl chloroform, vigorously shaken, and incubated for 10 min at RT. Then the reaction tubes were centrifuged for 15 min at 12000 x g at 4 °C. After this, each tube had three layers: the transparent top layer containing RNA, the interphase with the white precipitated DNA, and the pink organic bottom phase. The upper layer was carefully transferred into another new centrifuge tube and 250 µl of 100% isopropanol were added for each tube. After thoroughly mixing, the tubes were incubated at RT for 10 min. Then, they were centrifuged for 10 min at 12000 x g at 4 °C and the isopropanol was carefully pipetted out in order to avoid RNA pellets were lost. After washing, the pellet was immersed in 500 µl 75% ethanol, gently shaken, and recentrifuged at 12000 x g for 5 min. The ethanol was poured off and the pellets were air dried for 5 to 10 min. Finally, the pellets were resuspended in approximately 50-100 µl RNase-free water. The NanoDrop ND1000 spectrophotometer (Fisher NanoDrop, USA) was used to quantify total RNA concentration and quality. Afterward, the RNA samples were preserved at -80 °C until further usage.

2.9.2 Removal of genomic DNA

The DNase I Kit (Sigma-Aldrich Chemie GmbH, Germany) was used to eradicate genomic DNA from the extracted RNA of primary microglia cells. 1000 ng of total RNA was utilized, and DNA removal was carried out according to the kit instructions (Table 6). Afterwards,

samples were incubated for 30 min at 37 °C. 50 µL ethylenediaminetetraacetic acid (EDTA) was added to the samples to halt the process and then incubated at 65 °C for an additional 10 min. Reverse transcription was undertaken using the purified RNA.

Table 6: A Pipetting strategy for removing genomic DNA

Component	Volume
RNA	1 µg
10X Reaction Buffer with $MgCl_2$	1 µl
DNase I, RNase-free	1 µl
Water, nuclease-free	to 10 µl

2.9.3 Reverse transcription

200ng of template RNA was transcribed in a total of 12 µl with RevertAid H Minus First Strand cDNA Synthesis Kit (Fisher Scientific GmbH, Germany) according to the manufacturer's instructions (Table 7). All components were added to a sterile nuclease-free tube, which was quickly centrifuged and incubated at 65 °C for 5 min. The following components (Table 8) were then carefully added and then incubated at 42 °C for 60 min.

Table 7: First-strand cDNA synthesis

Component	Volume
Template	200 ng
Olido $(dT)_{18}$ primer	1 µl
Water, nuclease-free	to 12 µl

Table 8: First-strand cDNA synthesis

Component	Volume
5X Reaction Buffer	4 µl
RiboLock RNase Inhibitor (20 U/µl)	1 µl
10 mM dNTP Mix	2 µl

RevertAid H Minus M-MuL V Reverse Transcriptase (200 U/µl)	1 µl
Total volume	to 20 µl

2.9.4 Quantitative real-time PCR

The quantitative real-time PCR (qRT-PCR) reaction was carried out in accordance with the standard procedure (Table 9). In a total volume of 10 µl, the components were combined as described in Table 10 of LightCycler® 480 SYBR Green I Master reaction mix with the miRNA-specific forward primer and the universal reverse primer as stated in Table 11. The expression of peptidylprolyl isomerase A (PPIA) and GAPDH as housekeeping genes were quantified in 3 biological replicates for each experimental group and measured in 3 technical replicates. Graphpad Prism 9 (GraphPad Software, USA) was used to display all of the analysis for the comparable results according to the $2^{-\Delta\Delta Ct}$ method (Zhang L et al. 2021).

Table 9: Standard protocol for miRNA qRT-PCR reaction

Step	Description	Time and Temperature
1	Thermocycler protocol	5 min, 95 °C
2		10 sec, 95 °C
3		20 sec, 60 °C
4		10 sec, 40 °C
5	Melting curve evaluation	5 sec, 95 °C
6		1 min, 65 °C
7		continuous, 97 °C
	Number of cycles	40

Table 10: Pipetting scheme for miRNA qRT-PCR

Component	Volume
cDNA	2.5 µl
Forward Primer	0.5 µl

Reverse Primer	0.5 µl
LightCycler® 480 SYBR Green I Master	5 µl
DEPC water, RNase-free	1.5 µl

Table 11: Sequence information of qRT-PCR primers

Gene name	Sequence (5' - 3')
GAPDH	Forward Sequence: TGGATTTGGACGCATTGGTC
	Reverse Sequence: TTTGCACTGGTACGTGTTGAT
PPIA	Forward Sequence: GAGCTGTTTGCAGACAAAGTTC
	Reverse Sequence: CCCTGGCACATGAATCCTGG
NEAT1	Forward Sequence: GTAATTTTCGCTCGGCCTGG
	Reverse Sequence: TACCCGAGACTACTTCCCCA
TREM2	Forward Sequence: CCCACCTGGCTGTTGTCCTT
	Reverse Sequence: TCGCTACCGTGGAGGCTCTG
PLIN2	Forward Sequence: ACACCCTCCTGTCCAACATC
	Reverse Sequence: AAGGGACCTACCAGCCAGTT
Atg3	Forward Sequence: ACACGGTGAAGGGAAAGGC
	Reverse Sequence: TGGTGGACTAAGTGATCTCCAG
Atg5	Forward Sequence: TGTGCTTCGAGATGTGTGGTT
	Reverse Sequence: ACCAACGTCAAATAGCTGACTC
Beclin1	Forward Sequence: ATGGAGGGGTCTAAGGCGTC
	Reverse Sequence: TGGGCTGTGGTAAGTAATGGA
STAT3	Forward Sequence: CTTGTCTACCTCTACCCCGACAT
	Reverse Sequence: GATCCATGTCAAACGTGAGCG

TNF-α	Forward Sequence: AAGCCTGTAGCCCACGTCGTA
	Reverse Sequence: GGCACCACTAGTTGGTTGTCTTTG
IL-1β	Forward Sequence: GCAACTGTTCCTGAACTCAACT
	Reverse Sequence: ATCTTTTGGGGTCCGTCCAACT
IL-4	Forward Sequence: GCCACCATGAGAAGGACACT
	Reverse Sequence: ACTCTGGTTGGCTTCCTTCA
IL-10	Forward Sequence: AGAAAAGAGAGCTCCATCATGC
	Reverse Sequence: TTATTGTCTTCCCGGCTGTACT

2.10. Immunofluorescence

Primary microglia were seeded on slides at 1.5 x 10^4 cells/well density. The cells were put on ice after one day of culture and washed two times with ice-cold DPBS. Then, the cells were fixed for 15 min at RT using 4% formaldehyde and washed two times with DPBS. Afterward, a permeabilization step followed with 0.25% PBS-TritonX100 for 10 min and three subsequent washes with DPBS for 5 min each. Afterward, 10% donkey serum with 1% Bovine Serum Albumin (BSA) melted in DPBS was used for blocking and cultured for 1 hour at RT. The primary antibody was prepared and incubated overnight at 4 °C. The following day, the cells were washed three times with phosphate-buffered saline-Tween (PBST) for 5 min each wash to eliminate the unbound primary antibody. Then 250 µl of the fluor-secondary antibody was added and incubated for 1 hour. Finally, DAPI was applied, followed by one wash with PBST and two times with DPBS. The slides were mounted using Shandon™ Immuno-Mount™ and sealed with nail polish and then polymerized at 4 °C overnight for microscopy utilization. In particular, BODIPY-stained cells had to be washed with PBS and did not need secondary antibodies. The specific antibody working dilutions were given as follows: polyclonal rabbit anti-CD11b antibody (2 µg/ml; Abcam, UK), monoclonal rat anti-CD68 antibody (2 µg/ml; BioRad, USA), polyclonal rabbit CX3CR1 antibody (2 µg/ml; Thermo Fisher Scientific, USA), polyclonal rabbit anti-Iba1 antibody (2 µg/ml; Abcam, UK) and a stain for neutral lipids, BODIPY 493/503 (Thermo Fisher Scientific, USA). Cy-3 labeled or Alexa Fluor 488 labeled secondary antibody (1:10,000, Jackson Immuno, USA) was used to detect the primary antibody staining.

2.11. Cellular samples preparation for protein analysis

Primary microglia were seeded at 2 x 10^5 cells/well density. Different groups had undergone different treatments. Firstly, the cells were washed twice with ice-cold DPBS. Meanwhile, the mixed working buffer was prepared according to 1x radioimmunoprecipitation assay (RIPA): protease inhibitor cocktail (PIC): PhStop = 9.1: 0.4: 0.5. Then, each well was added with 85 µl of working buffer and placed on ice for 5 min. The cells were scraped off and pipetted up and down in the buffer. After that, cell lysates were transferred to a 1.5 ml tube and sonicated for 5 min in ice-cold water. Then the samples were centrifuged at 14000 x g for 10 min at 4 °C. Finally, the supernatant was gathered and kept at -80 °C for future experiments. Total protein samples were quantified based on the Pierce BCA Protein Assay Kit' s instructions (Thermo Fisher Scientific, USA). Afterwards, the final concentration of every sample was calculated based on a standard curve (0 ng/µl, 100 ng/µl, 200 ng/µl, 500 ng/µl, 1000 ng/µl, and 2000 ng/µl), and the corresponding absorbance. Then each sample was adjusted to the same concentration by adding cell lysate based on the measured protein concentration. After boiling for 10 min in a metal bath at 100 °C , the protein samples were placed on ice until further SDS-polyacrylamide gel electrophoresis (SDS-PAGE).

2.12. Western blot

SDS-PAGE gels consist of a lower layer of separation gel and an upper layer of stacking gel, with the separation gel being 10% or 15% depending on the molecular weight of the target proteins. The SDS-PAGE gels were prepared in accordance with the manufacturer's instructions. The protein samples were centrifuged and mixed in advance, and the samples were added in the corresponding gel lanes in turn with a pipette, followed by a 2 µl protein marker was added between the samples. The lid of the electrophoresis tank was placed on the positive and negative electrodes. Furthermore, the initial voltage of 55V was set to start electrophoresis. After the samples entered into the separating gel and the protein marker separated, the voltage was adjusted to 120V to continue electrophoresis until the bromophenol blue dye marker reached the bottom of the separating gel. After the electrophoresis, proteins were transferred to a polyvinylidene fluoride or polyvinylidene difluoride (PVDF) membrane using a semi-dry technique. First, the PVDF membrane were put with filter papers in the transfer buffer after activating it for 10 seconds in methanol. Afterwards, the infiltrated filter paper, the activated PVDF membrane, the gel, and the infiltrated filter paper were place in order in a semi-dry tank. A roller was used to eliminate air bubbles between the layers. Subsequently, after 1 hour of transfer at 400 mA, the

membrane was blocked with 5% skim milk dissolved in deionized water for 1 hour at RT. Then, the blocked PVDF membrane was washed in the membrane washing solution (Tris-buffered saline-Tween, TBST) three times on a shaker for 3 min each. Finally, the membrane was treated with the respective primary antibody (1:1000 in BSA) overnight at 4 °C. On the next day the primary antibody was recycled and stored in the -20 °C freezer. After washing the membrane three times with TBST, it was incubated with the respective HRP coupled secondary antibody (1:10000 in TBST solution) for 1 hour at RT. After that, the membrane was washed several times. Finally, the rinsed membranes were immersed in ECL chemiluminescence reagent before the blots were exposed to the imaging equipment ChemiDoc station (Biorad, USA). Image Lab Software was used to evaluate the data further. Table 12 lists the details of the used antibodies.

Table 12: Antibody information

Antibody	Concentration	Supplier	Cat. No.	Species
Anti-Tublin	1:1000	GeneTex, USA	GTX628802	mouse
Anti-GAPDH	1:1000	GeneTex, USA	GTX627408	mouse
Anti-TREM2	1:1000	ThermoFisher, USA	PA5-87933	rabbit
Anti-PLIN2	1:1000	ProGen, Germany	GP42	guinea pig
Anti-LC3	1:1000	Abcam, UK	ab128025	rabbit
Anti-p62	1:1000	Abcam, UK	ab109012	rabbit
Anti-rabbit	1:10000	Abcam, UK	ab97051	goat
Anti-mouse	1:10000	Abcam, UK	ab97023	goat
Anti-guinea pig	1:10000	Abcam, UK	ab6908	Goat

2.13. Co-culture of primary microglia and SH-SY5Y cells

Human neuroblastoma (SH-SY5Y) cells were seeded in 24-transwell inserts at 2 x 10^5 cells/well density, and the primary microglia were seeded in another 24-well plate at 4 x 10^4 cells/well density. After transfection of ASO NEAT1 or ASO Scramble was performed with primary microglia, the microglia were cultured in BSS0 and subsequently transferred to a hypoxic incubator, as mentioned before. Afterwards, microglia cells were co-cultured with SH-SY5Y cells in transwell plates for 24 hours. The supernatant was taken for further

analysis.

2.14. Statistical analysis

GraphPad Prism 9 software (GraphPad sofware, California, USA) was used for statistical analysis and graphic production, whereas Excel was utilized for data collection. One-way ANOVA followed by Tukey's post-hoc-test was explicitly chosen to compare multiple groups. All data are given as mean ± standard deviation (SD), and *p* values less than 0.05 was considered significant.

3. Results

3.1. Purification, isolation, and characterization of primary microglia

Cell morphology was observed under bright-field microscopy to identify primary microglia, and immunofluorescence was used against the markers of primary microglia. As presented in Figure 1, the primary microglia showed a ramified morphology.

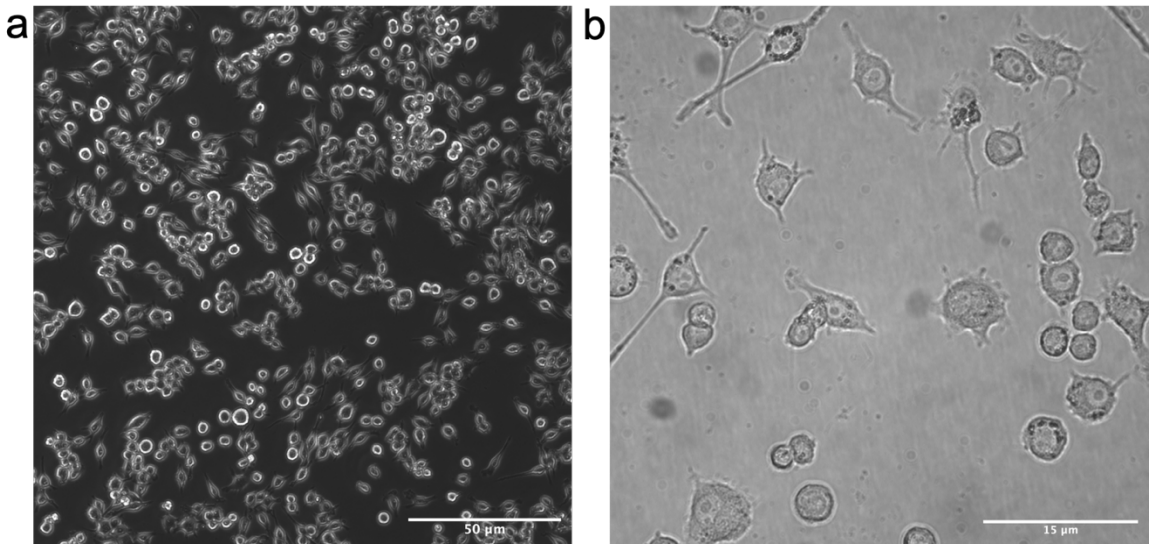

Figure 1: Morphology of primary microglia. a. Primary microglia cells were isolated from cerebral cortices and hippocampi of newborn WT C57BL/6J mice. The cells have a small soma bearing long and thin extensions. b. Primary microglia at higher magnification.

Four commonly-used microglia markers were analyzed by using fluorescence microscopes, namely CD68, CD11b, CX3CR1, and Iba1 (Figure 2).

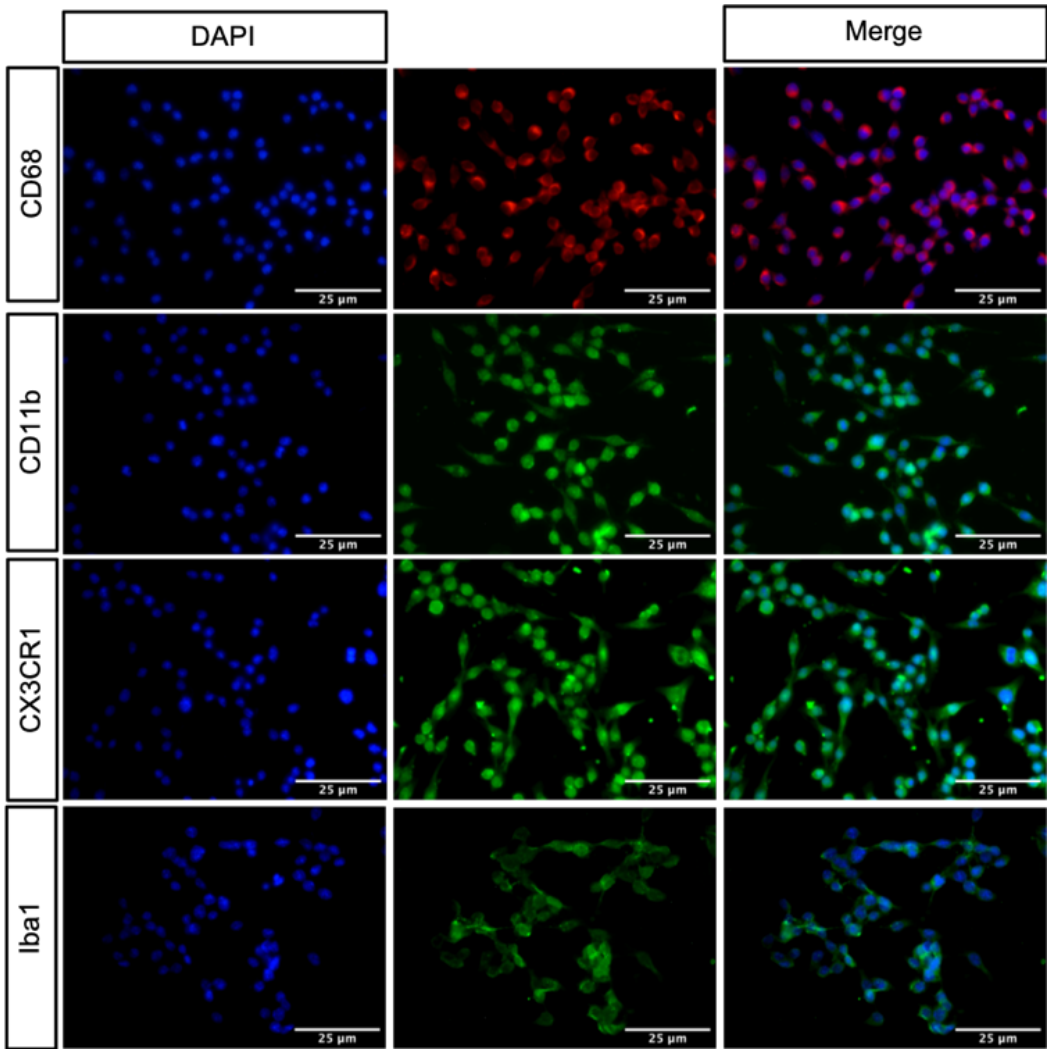

Figure 2: Identification of primary microglia. Immunofluorescence images labelled for CD68 in red and CD11b, CX3CR1, and Iba1 in green under normoxic conditions, while the nuclei were counterstained with DAPI in blue (top to bottom).

3.2. Establishment of an OGD model in vitro and NEAT1 expression in primary microglia under hypoxic conditions

Firstly, we discovered the expression of NEAT1 in the primary microglia under OGD conditions. After 24 hours of reoxygenation, RNA was extracted, and NEAT1 expression was measured. qRT-PCR findings revealed that the level of NEAT1 in the primary microglia of the OGD group was considerably higher than the normoxia group, as shown in Figure 3a. In addition, NEAT1 expression peaked after 4 hours of OGD and 24 hours of reoxygenation. The MTT assay was adopted to determine the cell viability at various time points. As shown in Figure 3b, the cell viability was affected after 2 hours of OGD and then gradually decreased around 50% compared to normoxia after 4 or 6 hours of OGD.

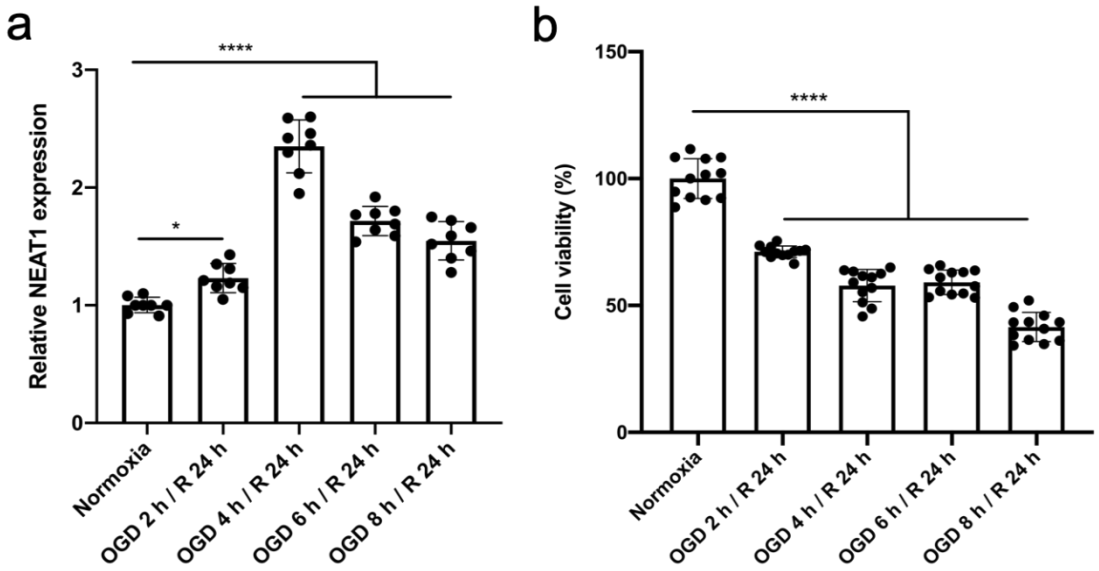

Figure 3: Establishment of OGD model and NEAT1 expression in primary microglia at different time points of OGD. a. NEAT1 expression was analyzed in primary microglia after 2, 4, 6, and 8 hours of OGD with 24 hours of reoxygenation using qRT-PCR normalized against PPIA. b. Effect of different time points of OGD with 24 hours reoxygenation on cell viability. * $p < 0.05$, **** $p <$ 0.0001 vs. corresponding control, ANOVA.

In order to further verify the function of NEAT1 in primary microglia, the expression of NEAT1 was measured by qRT-PCR between normoxia and 4 hours of OGD with 3, 6, 9, 12, 15,18, 21 and 24 hours of reoxygenation, respectively. Figure 4a showes that, compared to the control, the expression of NEAT1 in microglia reached the top after 6 hours of reoxygenation. The cell viability after different reoxygenation times is illustrated in Figure 4b. So the time point of 4 hours of OGD and 6 hours of reoxygenation was used in the subsequent experiments.

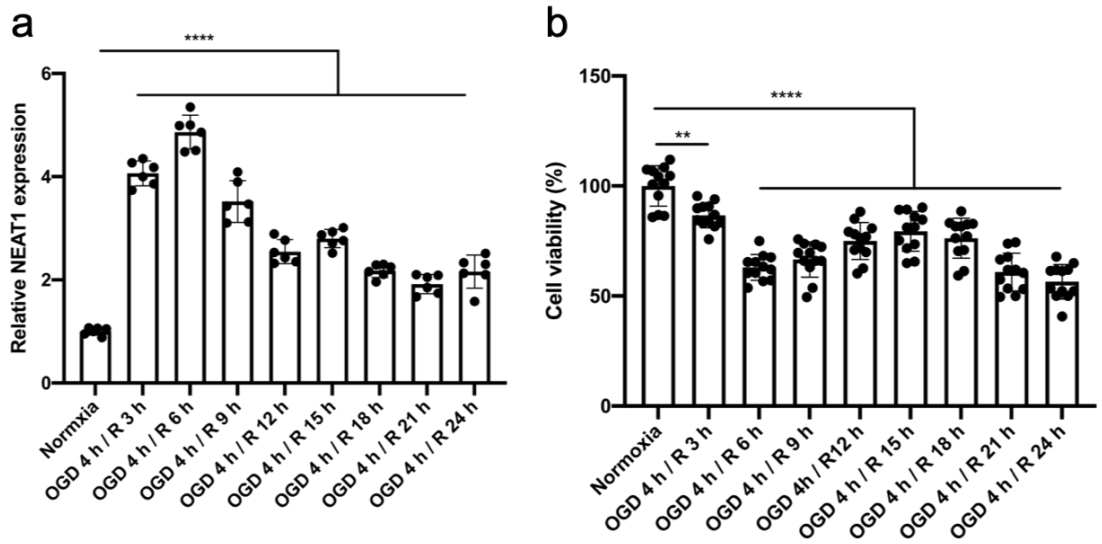

Figure 4: Relative NEAT1 expression in primary microglia at different time points after reoxygenation and relative cell viability. a. RNA was extracted from primary microglia cells after 4 hours of OGD with different times of reoxygenation, and NEAT1 expression was detected by qRT-PCR, normalized to PPIA. b. Effect of varied reoxygenation time points with 4 hours of OGD on cell survival. ** $p < 0.01$, **** $p < 0.0001$ vs. corresponding control, ANOVA.

3.3. The efficiency of NEAT1 knockdown and its effect on microglia viability

The cells were transfected with ASO NEAT1 of different concentrations, and transfection effectiveness was assessed by qRT-PCR (Figure 5). The results show that 80 nM were the best dosage (Figure 5b). At the same time, the cell viability was measured by the MTT test. Figure 5c displayed that the pre-treatment with ASO NEAT1 significantly increased the cell viability of microglia. At the same time, there is no significant difference between the OGD, blank control (Turbofect), and negative control (NC, ASO Scramble) groups.

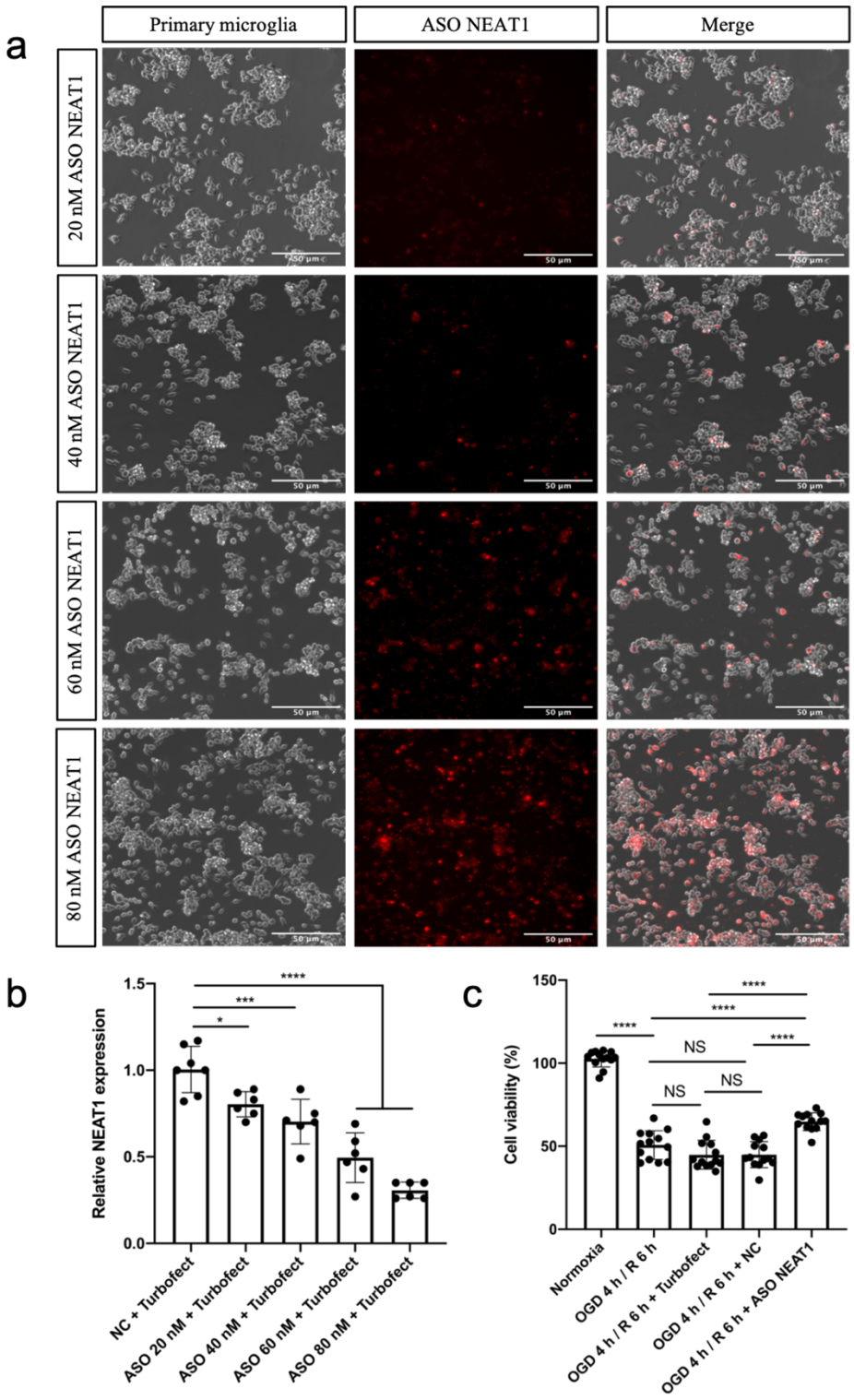

Figure 5: The transfection efficiency and cell viability of microglia treated with ASO NEAT1. a. Bright-field microscopy images of microglia cells transfected with ASO NEAT1 of different concentrations. b. The transfection efficiency of ASO NEAT1 was quantified by qRT-PCR and normalized to PPIA. c. Cell viabilities of microglia treated with ASO NEAT1 determined by MTT assay. Experiments were performed in five parallel groups. NS, not significant, * $p < 0.05$, *** $p < 0.001$, **** $p < 0.0001$ vs. corresponding control, ANOVA.

3.4. Knockdown of NEAT1 affects expression patterns of lipid droplet in primary microglia exposed to OGD

We first investigated whether knockdown of NEAT1 could affect the expression patterns of LDs in microglia under OGD conditions. According to the immunofluorescence results, a significant upregulation of LDs was expressed in microglia under OGD compared to the normoxic conditions (Figure 6). Subsequently, the cells were treated with ASO NEAT1 or Scramble, respectively, and the result demonstrated that knockdown of NEAT1 significantly inhibited the LDs expression in microglia.

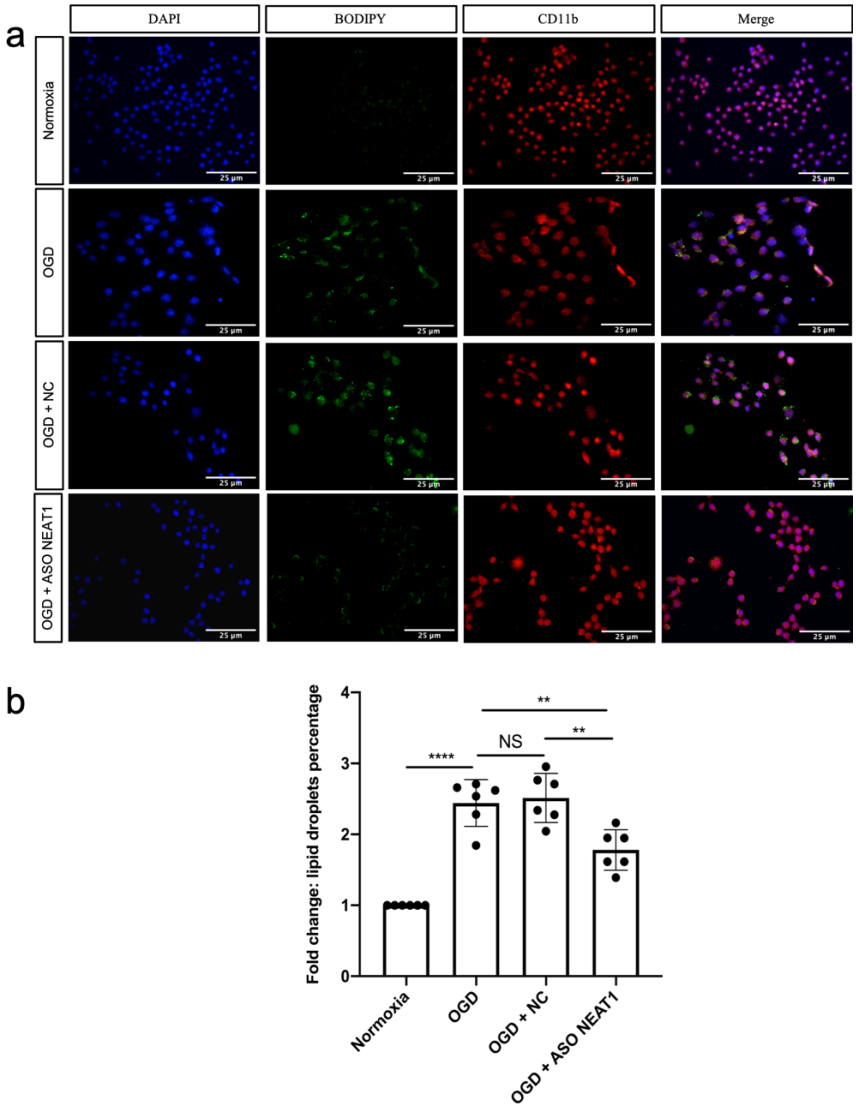

Figure 6: The effect of NEAT1 on lipid droplet accumulation in the primary microglia. a. Immunofluorescence staining of neutral LDs (BODIPY, green) in microglia cells (CD11b, red) cultured under normoxic and hypoxic conditions after interference with ASO NEAT1. b. Quantification of the fold change of LDs and statistical evaluation. NS, not significant, ** $p < 0.01$, **** $p < 0.0001$ vs. corresponding control, ANOVA.

After oxygen-glucose deprivation and reperfusion (OGD/R) treatment with the primary microglia, Perilipin 2 (PLIN2) and triggering receptors expressed on myeloid cells 2 (TREM2) were enhanced. Moreover, the knockdown of NEAT1 significantly downregulated PLIN2 and upregulated TREM2 expression, respectively, relative to the OGD group, while there was no significant difference between the OGD and negative control groups (Figure 7).

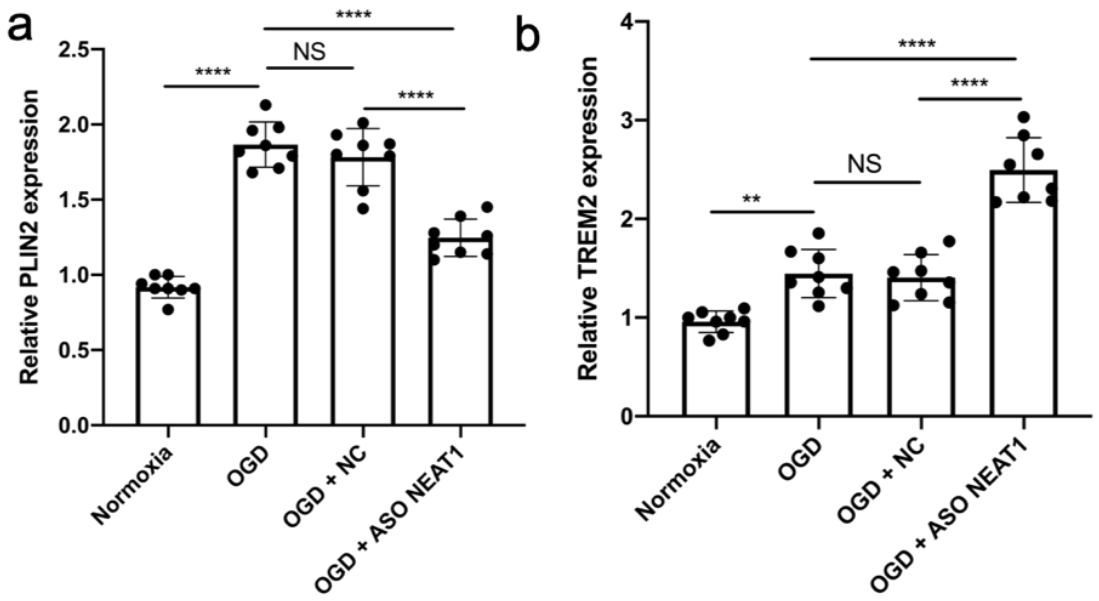

Figure 7: Relative expression of PLIN2 and TREM2 in primary microglia cells transfected with ASO NEAT1 or ASO Scramble. Primary microglia cells were transfected with ASO NEAT1 or Scramble for 24 hours to generate stable NEAT1 knockdown and negative control groups. qRT-PCR analysis was utilized to detect LD-related genes (a) PLIN2 and (b) TREM2 expression levels, normalized to PPIA. NS, not significant, ** $p < 0.01$, **** $p < 0.0001$ vs. corresponding control, ANOVA.

Inflammation has been hypothesized as both a cause and a consequence of LD formation. In order to further confirm the effect of NEAT1 on LDs, we tested the expression of inflammation-related genes via qRT-PCR after different treatments as mentioned before. As indicated in Figure 8, inflammation-related genes were upregulated after exposure to OGD as compared to the normoxic conditions. Knockdown of NEAT1 significantly downregulated TNF-α and IL-1β while upregulated IL-4 and IL-10 expression compared to the OGD group.

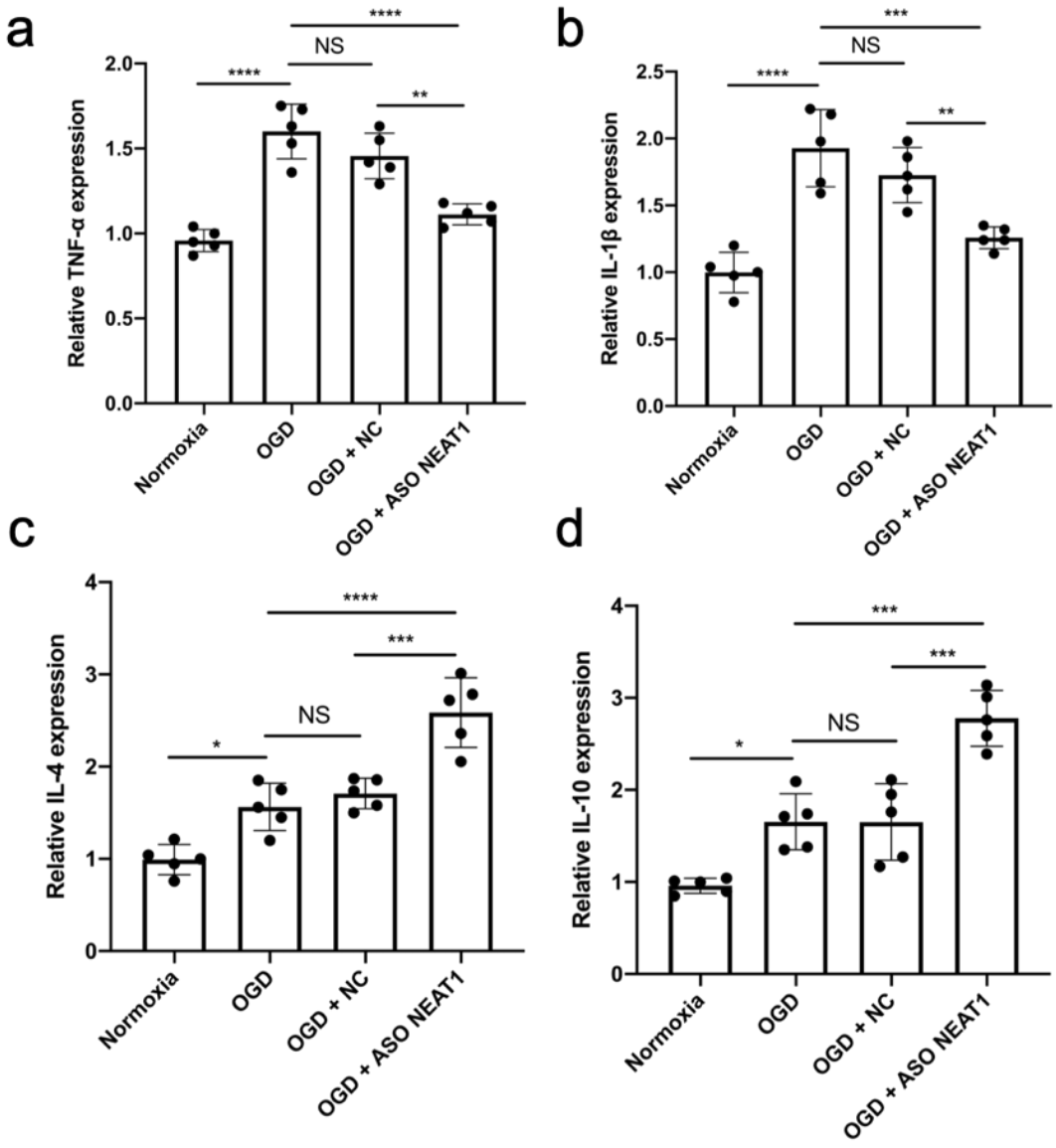

Figure 8: Relative expression of inflammatory markers in primary microglia cells transfected with ASO NEAT1 or ASO Scramble. Primary microglia cells were transfected with ASO NEAT1 or Scramble for 24 hours to generate stable NEAT1 knockdown and negative control groups. Detection of inflammation-related genes (a) TNF-α, (b) IL-1β, (c) IL-4, and (d) IL-10 levels were quantitated by qRT-PCR analysis, normalized to GAPDH. NS, not significant, * $p < 0.05$, ** $p < 0.01$, *** $p < 0.001$, **** $p < 0.0001$ vs. corresponding control, ANOVA.

To further confirm that knockdown of NEAT1 could repress the LD accumulation in microglia cells exposed to OGD, we performed western blots to analyze the LDs-associated proteins, PLIN2 and TREM2. As Figure 9 shows, the expression of PLIN2 and TREM2 was significantly increased under OGD compared to normoxic conditions. Compared to the negative control group, PLIN2 decreased, while TREM2 was significantly increased in the ASO NEAT1 transfected cells.

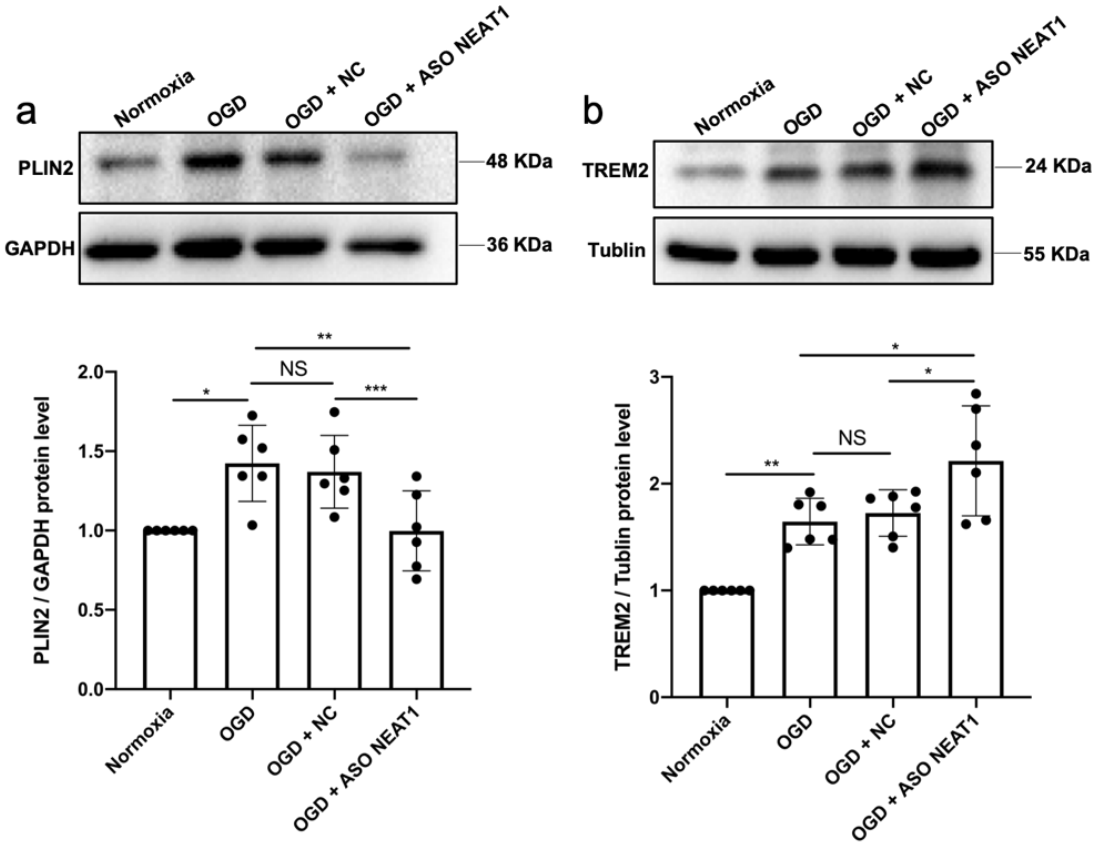

Figure 9: NEAT1 knockdown repressed PLIN2 but activated TREM2 expression. Microglia cells were transfected for 24 hours with ASO NEAT1. Western blot analysis was used to assess the expression of (a) PLIN2 and (b) TREM2 in microglia cells in four parallel groups (Normoxia, OGD, OGD + NC, and OGD + ASO NEAT1), and the relative quantitative analysis was normalized against GAPDH or tublin, as indicated. NS, not significant, * $p < 0.05$, ** $p < 0.01$, *** $p < 0.001$ vs. corresponding control, ANOVA.

3.5. Knockdown of NEAT1 affects signaling cascades related to autophagy in primary microglia under ischemic conditions

To determine the impact of NEAT1 on the autophagy pathway, we treated microglia with ASO NEAT1 or ASO Scramble at a concentration of 80 nM/well, respectively. The results demonstrate that NEAT1 silencing significantly reduced mRNA levels of Atg3, Atg5, Beclin1, STAT3, as well as protein level of LC3 while increasing the protein level of p62 in microglia cells compared to the OGD group, as illustrated in Figures 10 and 11. These findings show that the knockdown of NEAT1 impairs the autophagy process in primary microglia under OGDconditions.

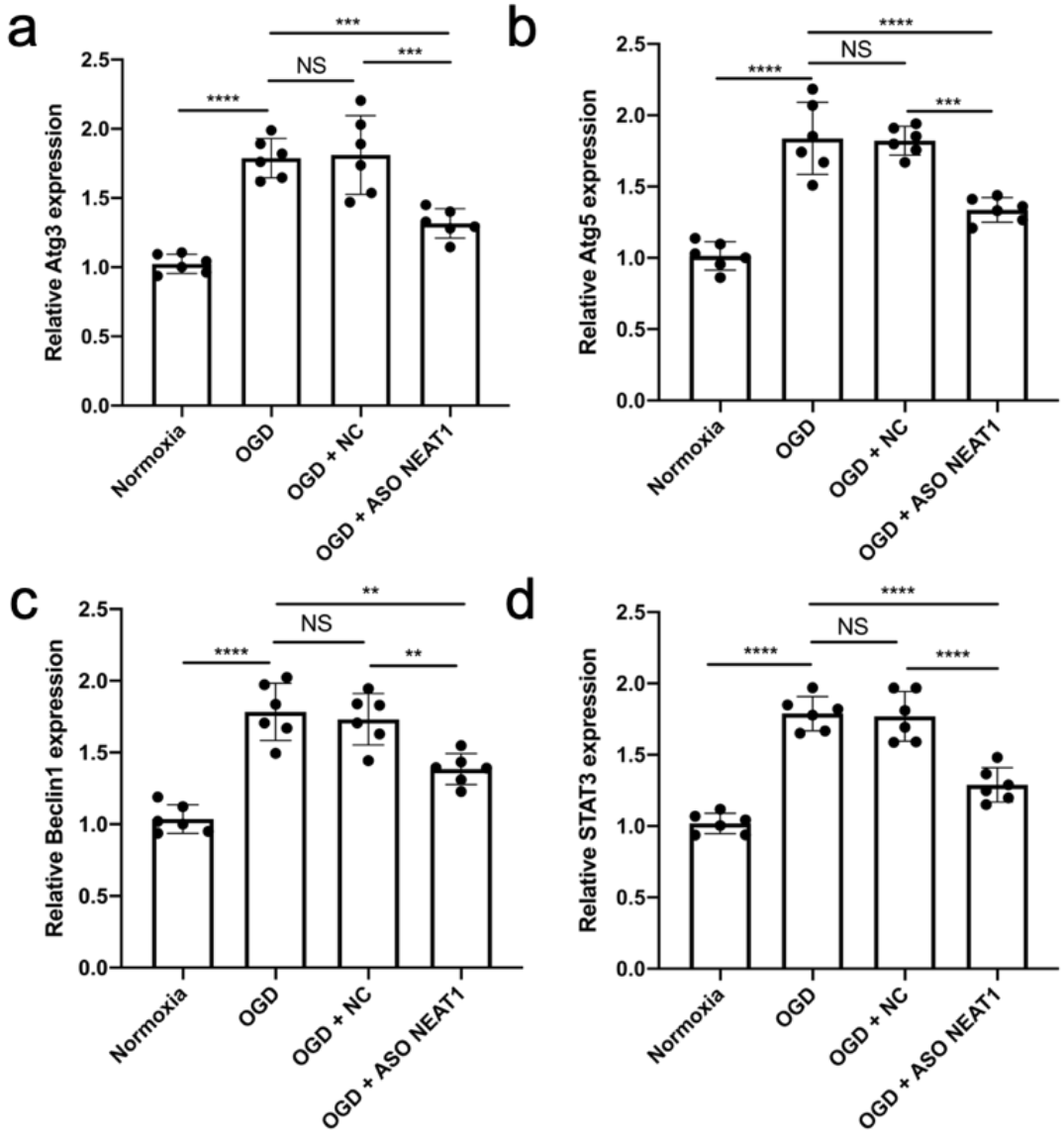

Figure 10: Relative expression of autophagy-related genes in microglia transfected with ASO NEAT1 or ASO Scramble. Primary microglia cells were transfected with ASO NEAT1. Autophagy-related genes were determined by quantitative qRT-PCR. Analysis of (a) Atg3, (b) Atg5, (c) Beclin1, and (d) STAT3 using qRT-PCR normalized to GAPDH. NS, not significant, ** $p < 0.01$, *** $P < 0.001$, **** $p < 0.0001$ vs. corresponding control, ANOVA.

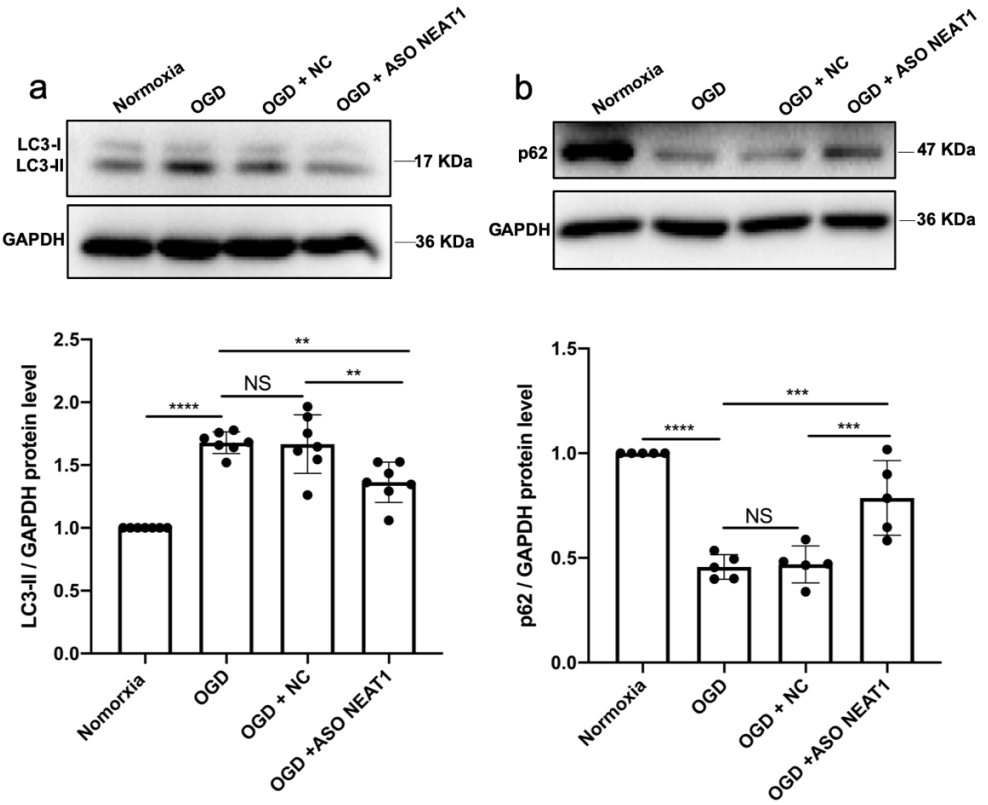

Figure 11: NEAT1 knockdown repressed LC3 but activated p62 expressions. Microglia cells were transfected with ASO NEAT1. Western blot was utilized to analyze the expression of (a) LC3 at a 17 kDa band and (b) p62 at a 47 kDa band in microglia cells in four parallel groups (Normoxia, OGD, OGD + ASO NC, and OGD + ASO NEAT1), and the relative quantitative analysis was normalized against GAPDH. NS, not significant, ** $p < 0.01$, *** $p < 0.001$, **** $p < 0.0001$ vs. corresponding control, ANOVA.

3.6. Inhibition or activation of the autophagy pathway affects lipid droplet formation in primary microglia

As stated earlier, NEAT1 and LD expression in microglia under OGD conditions were elevated, and silencing NEAT1 restricted both expression patterns of LDs and signaling cascades related to autophagy. In order to illustrate the interaction of autophagy and LDs accumulation, we next used 3-methyladenin (3-MA) and RAPA to inhibit or activate the autophagy pathway in microglia cells. 3-MA is a class III PI3K inhibitor that can specifically disrupt the fusion of autophagic vesicles and lysosomes during autophagy, whereas RAPA stimulates autophagy. Firstly, we stained the LDs accumulation in cells under normoxic conditions. Figure 12 demonstrated that with the addition of RAPA, the expression of LDs in the normoxia + RAPA group increased in comparison to the normoxia group, and the difference was statistically significant. There was no variation among the normoxia and normoxia + 3-MA or normoxia + DMSO groups.

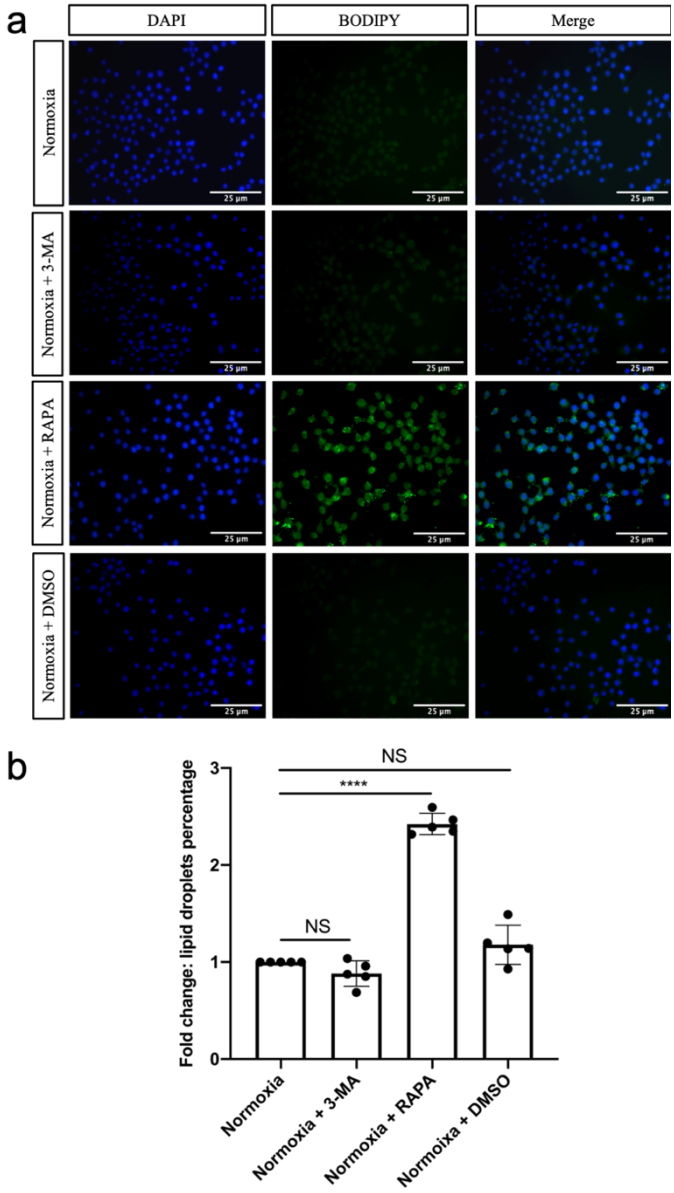

Figure 12: The staining of LDs in primary microglia after inhibition or activation of the autophagy pathway under normoxic conditions. a. Microglia cells were treated with 3-MA or RAPA for 24 hours, followed by BODIPY staining. b. Quantification analysis of the fold change of LDs. NS, not significant, **** $p < 0.0001$ vs. corresponding control, ANOVA.

Next, we stained the LD accumulation in microglia cells under OGD conditions. The results (Figure 13) show that after the treatment with 3-MA or RAPA, the proportion of green fluorescence signal in the cells was significantly decreased or increased, respectively. Furthermore, RAPA reversed the decreased LD accumulation induced by ASO NEAT1 upon OGD/R in microglia, whereas 3-MA had the opposite effect. In addition, there was no statistical significance between the OGD + RAPA + ASO NEAT1 and OGD + DMSO + NC groups.

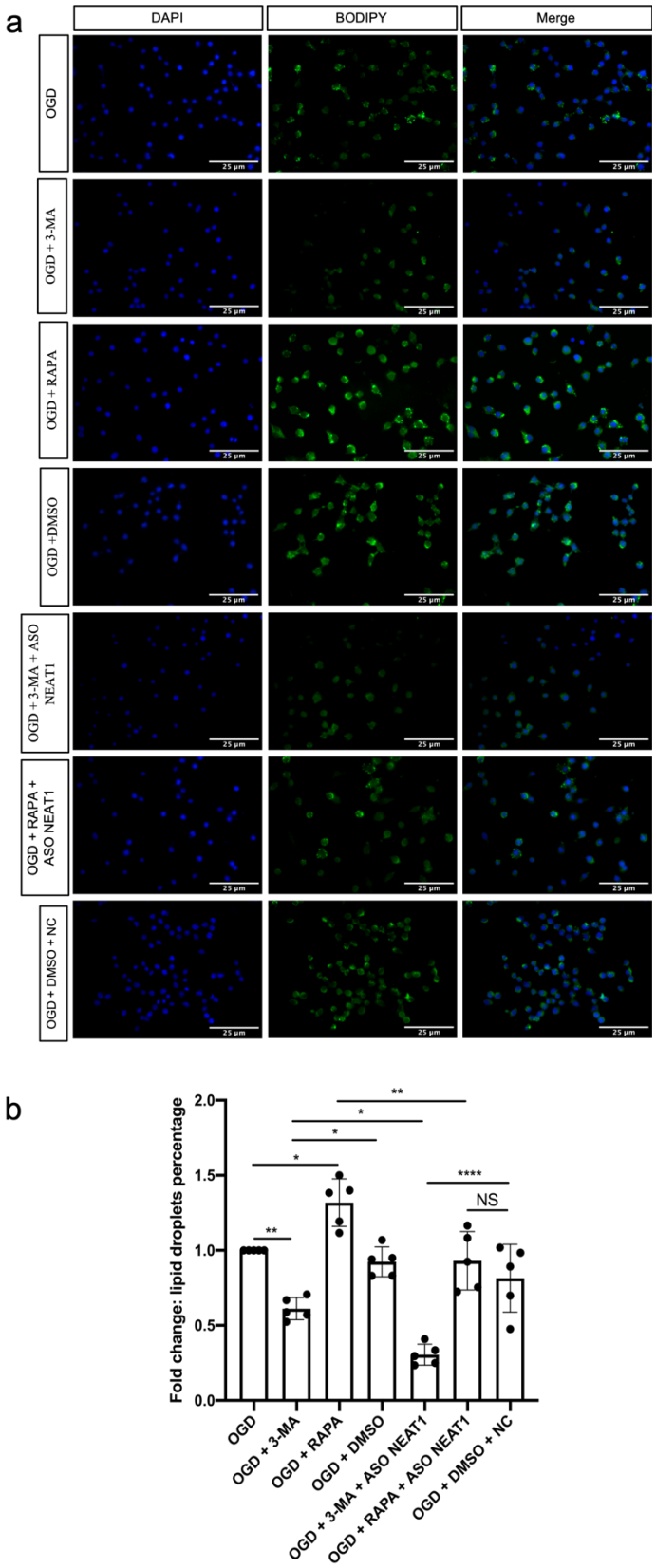

Figure 13: The staining of LDs in primary microglia after inhibition or activation of the autophagy pathway under OGD conditions. a. Microglia cells were treated with 3-MA or RAPA for 24 hours, followed by BODIPY staining b. Quantitative analysis of the fold change of LDs. NS, not significant, * $p < 0.05$, ** $p < 0.01$, **** $p < 0.0001$ vs. corresponding control, ANOVA.

To further demonstrate the interaction between autophagy and LD accumulation, the mRNA and protein levels of PLIN2 in microglia cells treated with 3-MA or RAPA under OGD conditions were analyzed. Similarly, the real-time PCR and western blot analyses demonstrated the same result, as shown in Figures 14 and 15.

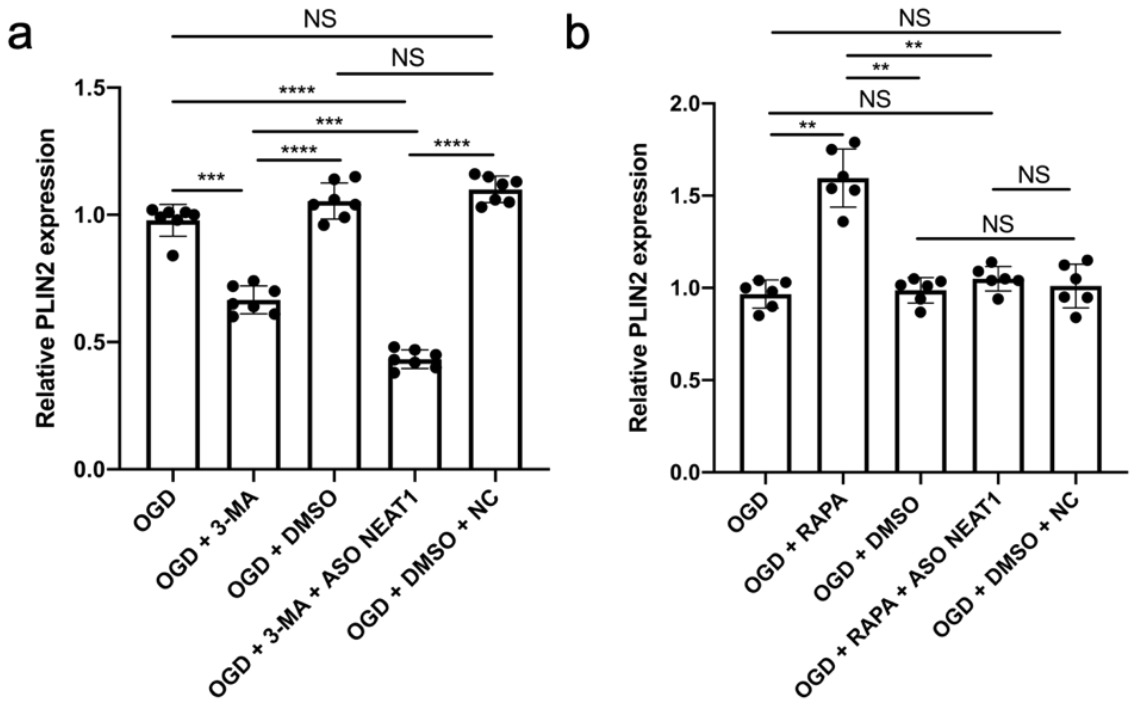

Figure 14: Relative PLIN2 gene expression in microglia cells after inhibition or activation of the autophagy pathway under OGD conditions. The expression level of PLIN2 treated with (a) 3-MA or (b) RAPA in microglia, normalized to PPIA. NS, not significant, ** $p < 0.01$, *** $p < 0.001$, **** $p < 0.0001$ vs. corresponding control, ANOVA.

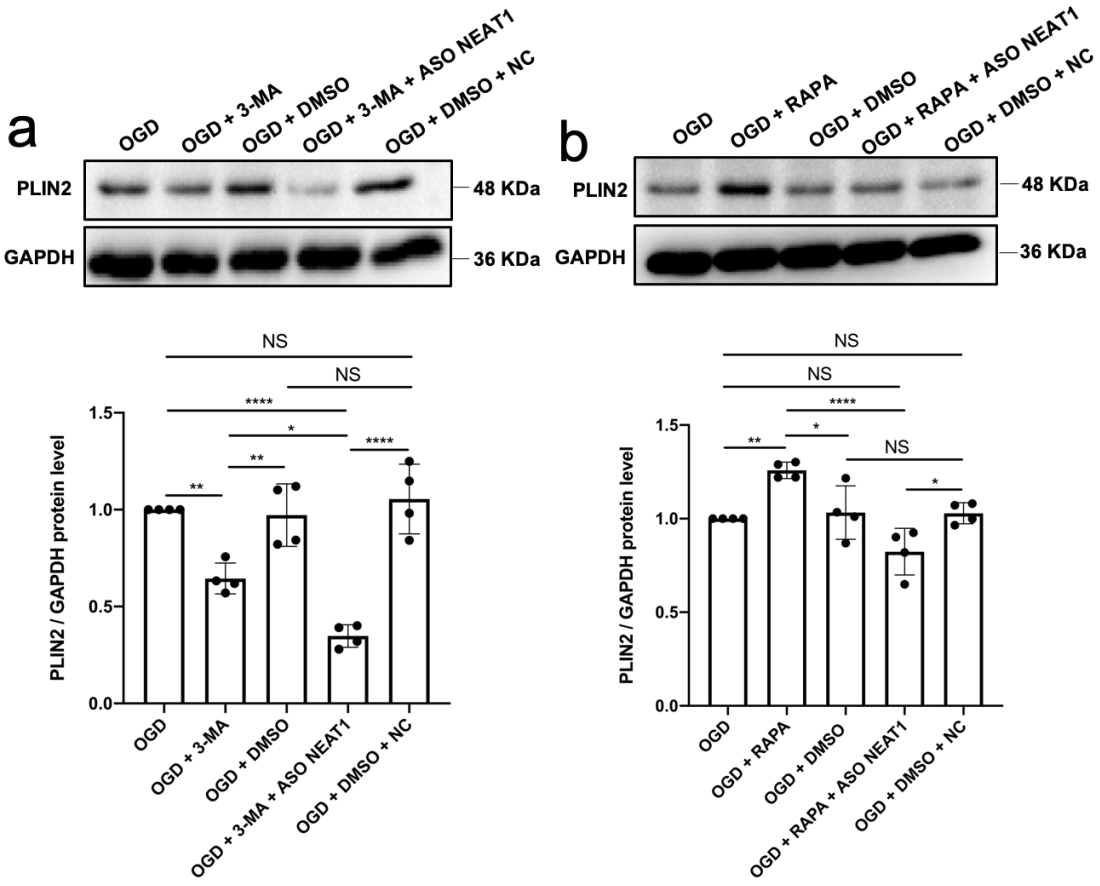

Figure 15: Protein level of PLIN2 in microglia after inhibition or activation of the autophagy pathway under OGD conditions. PLIN2 protein was recognized as a 48 kDa band, and GAPDH (36 kDa) was used as a reference. NS, not significant, * $p < 0.05$, ** $p < 0.01$, **** $p < 0.0001$ vs. corresponding control, ANOVA.

3.7. Knockdown of NEAT1 protects SH-SY5Y cells from OGD-injury

24 hours after ASO NEAT1 transfection into microglia cells, the cell viability was determined by MTT assay after cell co-culture (Figure 16a). The results show (Figure 16b) that the cell survival rate of SH-SY5Y cells in a total of three groups (co-culture + microglia OGD, co-culture + microglia NC, co-culture + microglia ASO NEAT1) was significantly higher than in the OGD group. Moreover, the cell survival in the co-cultured group of NEAT1 knockdown was improved as compared with the co-cultured group of OGD, and the difference was statistically significant ($P < 0.05$). There was no significant difference between the two groups "co-culture + microglia OGD" and "co-culture + microglia NC". These results indicate that primary microglia cells have an impact on SH-SY5Y cell viability amplified by the suppression of NEAT1 expression.

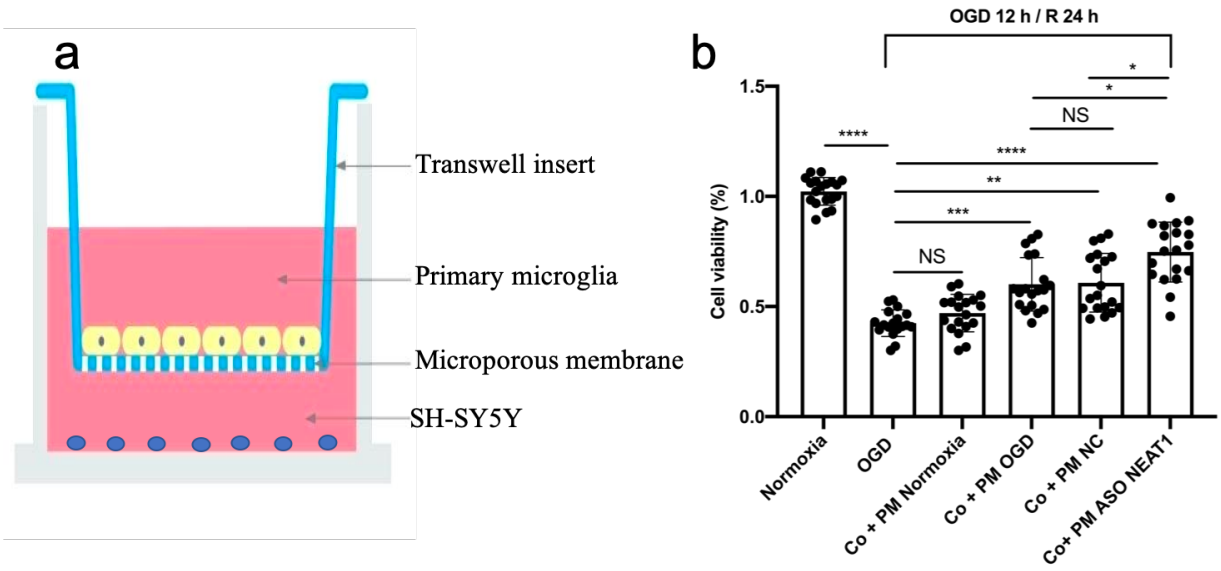

Figure 16: The cell viability of SH-SY5Y cells co-cultured with different groups of primary microglia. a. Schematic diagram of co-culture model. b. Cell viabilities of SH-SY5Y cells under normoxia, OGD, or co-cultured with groups of microglia determined by MTT assay. Experiments were performed in six parallel groups. NS, not significant. * $p < 0.05$, ** $p < 0.01$, *** $p < 0.001$, **** $p < 0.0001$ vs. corresponding control, ANOVA.

4. Discussion

Stroke is a CNS disease with acute onset, long-term disability, and even death. At present, the clinical treatment of stroke is still facing significant challenges. LncRNAs have been recognized as central mediators in various biological processes and have emerged as essential players in the control of ischemic diseases lately. This study looked at the involvement of NEAT1 in ischemic stroke and its downstream molecular regulatory mechanisms.

4.1. Identification of primary microglia, and establishment of OGD model in vitro

Cell culture in vitro is a method used to study the growth, proliferation, differentiation, and other functions of living cells. It has become a standard primary method in scientific research since the culture conditions can be easily controlled and are suitable for detection and recording. The CNS is comprised of two different kinds of cells: neurons and glial cells. The glial cells, mainly composed of microglia, astrocytes, and oligodendrocytes, account for more than half of the total cells and are essential for neural development and physiological functions (Huang H. et al. 2022). Astrocytes provide nutrition, support, and protection to neurons (Lee et al. 2021). Oligodendrocytes form neuronal myelination that wraps around neuronal axons, acting as an electric insulator to provide insulation and protection to neurons (Stadelmann et al. 2019). As resident immune cells, microglia can immunize, repair and maintain the homeostasis of the CNS, and play a vital role in mediating inflammatory response (Huang H et al. 2022).

In this study, to investigate the corresponding response after cerebral ischemia, the aim was to observe the physiological characteristics of microglia in vitro. The advantage of the in vitro approach is that the effects of other factors on cells, as compared to animal models, can be excluded, and the effect of a single factor on a single cell can be more easily observed and detected. The mouse age used in this experiment is a crucial factor affecting cell survival and purity (Woolf et al. 2021). The adhesion ability of the isolated cells becomes more robust from the younger animals, and better target cells needed for the experiment can be separated. Related studies have reported that cells isolated from newborn mice or fetal mice within one day have a more vital survival ability. The cerebral cortex of mice was preserved as much as possible since the microglia needed for the experiments are primarily located in the brain's gray matter. The brainstem and cerebellum were removed to the maximum in the process of isolation. Discarding the excess brainstem and cerebellum before cell isolation can avoid the

interference of unrelated tissues and enable experiments to obtain the highest purity of target cells possible (Lian H. et al. 2016). Secondly, the brain surface's meningeal tissue and related blood vessels had to be removed during the separation process to minimize the influence of vascular endothelial cells, leptomeningeal cells, and fiber cells on the target cells (Lian H. et al. 2016). Microglial cells with good activity and high purity were obtained by this approach, and the microglial cell-specific surface markers CD11b, CD68, CX3CR1, and Iba1 were confirmed by fluorescence microscope (Figure 2). Experiments showed that most cells were microglia, which laid the foundation for the next experiment.

A steady supply of oxygen and glucose is essential for maintaining proper brain activity (Watts et al. 2018). Recent research has demonstrated that the OGD/R treatment in vitro can simulate the process of ischemic injury in animals, involving apoptosis, mitochondrial dysfunction, oxidative stress, gene expression modulation, and other processes which can trigger neuronal death and brain injury (Zhang H et al. 2020). An MTT assay was performed to measure cell viability in order to further elucidate the influence of OGD/R on the survival rate of microglia at different time points. The underlying principle is that MTT can be reduced to a blue-purple formazan crystal under the action of succinate dehydrogenase in the mitochondria of living cells that cannot be dissolved in water and accumulates in the cell. However, dead cells cannot reduce MTT. Therefore, they cannot metabolize and degrade the materials. After forming the formazan, it was dissolved by the use of DMSO. The viability or number of living cells was then calculated by measuring the absorbance with a microplate reader. MTT detection has been widely used in life science because of its convenience and economy (Präbst et al. 2017). In this experiment, we found that after 2 hours of OGD, the cell survival rate of microglia cells started to be affected. The cell survival rate gradually decreased with the prolongation of OGD time. The results suggest that microglia are highly sensitive to oxygen and glucose conditions. When the microenvironment is hypoxic, the survival rate of microglia will decline sharply in a short period (Fumagalli et al. 2015).

4.2. NEAT1 and lipid droplet are upregulated in microglia exposed to OGD

Notably, the regulatory role of lncRNA-NEAT1 in cerebral ischemia has already been reported (Jin F et al. 2021; Liu B et al. 2020; Shen S et al. 2020). In this study, to clarify the NEAT1 expression under hypoxic conditions, OGD/R treatment with mouse-isolated primary microglia cells in vitro studies was performed. The relevant gene levels in the

OGD/R model was evaluated using qRT-PCR analysis. It was found that the expression of NEAT1 got the highest level after 4 hours of OGD and 6 hours of reoxygenation. Studies have reported that NEAT1 is upregulated in patients with acute ischemic stroke compared to healthy volunteers, and its expression is also favorably associated with inflammatory factors level (Li P et al. 2020). In addition, NEAT1 is a novel genetic phenotype of brain diseases and can facilitate the progression and invasion of glioma cells (Liang et al. 2022). Moreover, lentivirus transfection with NEAT1 overexpression exacerbated brain cell death in MCAO rats and significantly aggravated the cerebral IRI-induced nervous system injury on brain function after ischemic stroke (Shen S et al. 2020). Down-regulation of NEAT1 expression protected neurons against apoptosis caused by OGD/R in BV2 microglia cells, which significantly inhibited the polarization of microglia to the M1 phenotype (Ni et al. 2020). Besides, NEAT1 has been shown to function as a miR sponge to modulate the inflammatory response generated by OGD/R injury through miR-374a-5p/NFAT5 signaling pathway (Lian und Luo 2021). Consistent with this, the elevated level of NEAT1 in OGD/R-treated primary microglia cells found in this study indicates that NEAT1 plays a crucial function in IRI.

Microglia are the first immune cells to respond to brain damage and are triggered by blood components such as red blood cells, white blood cells, and plasma proteins (Kreutzberg 1996). Microglia act as the macrophages in the CNS by clearing denatured nervous tissue and infectious substances, thereby promoting neurological function recovery and maintaining the homeostasis of the CNS (Perry und Teeling 2013). However, in this process, activated microglia can also release a number of harmful cytokines, including pro-inflammatory cytokines, inflammatory mediators, reactive oxygen species (ROS), proteases, and nitric oxide synthase, which can aggravate the neurological injury caused by ischemia (Xin et al. 2021). Some studies have observed that neurodegenerative changes accompany significant accumulations of LDs in microglia under transmission electron microscopy (Shimabukuro et al. 2016). Lin et al. found that the number of microglia containing LDs was increased after glucose-oxygen-serum deprivation by Oil Red O-positive staining (Lin et al. 2019). Chemical blocking and antagonist experiments further demonstrated that peroxisome proliferator-activator receptor γ partially promotes LDs formation. The upregulation of LDs was accompanied by the increased production of inflammatory cytokines, tumor necrosis factor-α (TNF-α), and interleukin-1β (IL-1β). Inhibition of LDs formation significantly reduced the infarct size and improved the motor function deficit in rats with cerebral ischemia (Lin et al. 2019). One study using BODIPY staining found that the accumulation of LDs in microglia

significantly increased with age (Marschallinger J et al. 2020). RNA-sequencing differential expression analysis and the functional study suggested that LDs in these microglia were involved in the activation of ROS generation, which was related to the excessive release of pro-inflammatory factors and impaired phagocytosis of microglia (Marschallinger J et al. 2020). Similarly, in this study, performed immunofluorescence, qRT-PCR, and western blot analysis of LDs-related markers of primary microglia cells after exposure to hypoxia was performed and found that their expression is all elevated. Therefore, the LDs in microglia under hypoxic conditions are upregulated, possibly through induced and released pro-inflammatory factors or by lysosome and phagosome pathways. However, how LDs accumulate in hypoxic microglia and how they affect stroke progression is still unclear and needs further exploration.

4.3. NEAT1 affects the expression patterns of lipid droplet

Preliminary studies have revealed that the expression of NEAT1 and LDs is elevated in hypoxic microglia cells. NEAT1 was shown to be an upstream regulator of has-miR-372-3p, which involved RAPA-induced triglycerides (TGs) metabolism (Fan et al. 2021). NEAT1 also modulated adipose triglyceride lipase (ATGL) expression, and knockdown of it attenuated human hepatocellular carcinoma cell growth through ATGL (Liu X et al. 2018). TGs are the main contents of LDs, while ATGL is the primary enzyme contributing to TGs breakdown in vitro, so the aim of this study was to investigate whether NEAT1 has a specific effect on LDs metabolism. In this study, we inferred that the knockdown of NEAT1 could reduce LDs deposition in microglia after exposure to hypoxia. This conclusion agrees with some studies suggesting that NEAT1 may regulate lipid uptake in macrophages. For example, Ning et al. used oxidized low-density lipoprotein to acquire lipid absorption in macrophage THP-1 cells. The results indicated that the NEAT1 expression level was significantly increased compared with the normoxia group and further confirmed that low-level NEAT1-mediated paraspeckle formation suppressed lipid uptake (Huang-Fu et al. 2018). Silencing of NEAT1 expression by transfection with small interfering RNA can significantly prevent total cholesterol (TC), total TGs levels, and THP-1 cell death (Wang L et al. 2019). Microglia are the only macrophage population in the CNS, and one can assume that NEAT1 may affect expression patterns of LDs in primary microglia exposed to hypoxia. In addition, in specific fatty liver cells, NEAT1 interaction with downstream markers to adjust lipid metabolism has been demonstrated (Jin S et al. 2022).

In inflammation, LDs have long been considered to respond to inflammatory activation. Microglia show various forms of polarized activation during inflammation, one of which is typical M1 activation, which is characterized by driving the inflammatory response and possibly aggravating neuronal damage (Wendimu und Hooks 2022). M2 activation, on the other hand, limits excessive immune reactions, stimulates neuronal regeneration, and repairs damage (Guo et al. 2022). According to recent research, converting M1 to M2 might be a possible treatment method for ischemic injury (Wang J et al. 2018). The dynamics of microglial polarization reveal a novel mechanism for cerebral infarction. A rising number of studies have shown that the excessive release of inflammatory cytokines in ischemia-reperfusion and subsequent secondary inflammatory responses are the leading causes of brain injury and the development of revascularization (Halladin 2015). TNF-α, IL-1β, and IL-6 are inflammatory cytokines involved in the ischemia-reperfusion process, forming an inflammatory cascade (Qin et al. 2019). NEAT1 has been previously linked to the inflammatory response following cerebral ischemia-reperfusion. Ni et al. showed that NEAT1 suppressed the microglial polarization towards the M1 phenotype but did not promote the conversion to the M2 phenotype under hypoxia conditions (Ni et al. 2020). In addition, earlier studies have demonstrated that NEAT1 can regulate the blood-brain barrier damage induced by bacterial meningitis, and this process was mediated by miR-135a (Wang C et al. 2021). NEAT1 has already been shown to be an essential regulator of inflammatory processes in human tissues (Pan et al. 2021). Furthermore, NEAT1 is also emerging as a promising target for stroke therapy and has become a key actor as a diagnostic biomarker in the pathophysiology of cerebral infarction (Li P. et al. 2020). Silencing NEAT1 could significantly reduce proinflammatory cytokine production and alleviate ischemic damage in animal models (Jin F et al. 2021). These findings suggest that NEAT1 may reduce the inflammation reaction and further inhibit LDs accumulation indirectly. Consistent with this, in this study, changes in TNF-α, IL-1β, IL-4, and IL-10 expression after hypoxia were detected, and the results show that they were improved compared with the normoxia group. Then, after the knockdown of NEAT1, TNF-α and IL-1β were obviously down-regulated while IL-4 and IL-10 were up-regulated compared to the OGD group, further indicating the involvement of NEAT1 in inflammatory regulation.

4.4. NEAT1 affects signaling cascades related to autophagy

Autophagy is a critical degradation system for energy and cellular homeostasis, primarily as a defense mechanism that may prevent cell death in a stressful environment (Murrow und

Debnath 2013). At the same time, autophagy promotes survival or death in brain IRI, which is seen as a double-edged sword (Chen W et al. 2014). Wang et al. discovered that NEAT1 revealed decreased expression in the early phase of Alzheimer's disease and confirmed that NEAT1 could regulate Aβ uptake and degradation mediated by neuroglial cells through regulation of endocytosis-related gene expression (Wang Z et al. 2019). Further, they also proved that NEAT1 could induce autophagy in neuroglia cells via regulating autophagy-related gene expressions, such as Atg3, Atg5, and Beclin1 (Wang Z et al. 2022). Moreover, NEAT1 can stimulate autophagy in the progression of numerous diseases. For example, NEAT1 promotes myocardial IRI in diabetic rats by promoting myocardial autophagy (Ma et al. 2018). In the neurotoxin MPTP-induced Parkinson's disease model, NEAT1 aggravates autophagy (Dong et al. 2021; Yan et al. 2018). LC3-I and LC3-II bind together during autophagosome formation. In addition, LC3-I is found in the cytoplasm, whereas LC3-II is found in the autophagosome membrane. LC3-II is degraded with the autophagosome after fusion with lysosomes. The complete form of LC3 is representative of autophagy flux (Tanida et al. 2004).

In this study, autophagy was activated in OGD/R-treated microglia cells under OGD conditions, accompanied by upregulation of LDs and decreased cell proliferation. The increased expression of NEAT1 significantly promoted the transformation of LC3-I to LC3-II in microglia. Autophagy is a dynamic process, increased LC3-II/LC3-I ratio can only indicate increased autophagosomes (Singh und Bhaskar 2019). However, the increase in autophagosomes is not only due to the improvement of autophagy activity, but also may be caused by the blocked binding of autophagosomes and lysosomes or the degradation of autophagosomes. Therefore, we also detected the expression level of p62. The results show that NEAT1 knockdown up-regulated p62 expression. As p62 is an adaptor protein, one end of p62 connects explicitly to the LC3 protein on the autophagosome membrane, which acts as a membrane receptor, mediating the selective "packaging" process of the autophagosome membrane. The other end of p62 connects to the marked "cargo" through ubiquitin, and finally, the adaptor protein and "cargo" are degraded together. Therefore, the p62 protein level is negatively correlated with autophagy activity within a specific range, which is another marker in the process of autophagy (Jiang und Mizushima 2015). The level of p62 protein reflects the level of autophagosomes that are cleared. However, p62 accumulates when there is too much autophagy or insufficient clearance of autophagosomes (Jiang und Mizushima 2015). By detecting the expression of the aforementioned two markers, the results indicated that NEAT1 knockdown reduces autophagosome formation and inhibits autophagy activity.

Therefore, this infers that inhibition of NEAT1 expression can reduce the autophagy activation of microglia after exposure to hypoxia, reduce ischemia injury, and thus promote neuroprotection.

4.5. Inhibition or activation of the autophagy pathway affects lipid droplet formation in primary microglia

Mitochondria autophagy, ER autophagy, and peroxisome autophagy are found in cells (Xu et al. 2020). The fact that LDs are part of the cytoplasm and contain acid lipase within lysosomes suggests that the autophagy pathway can also degrade LDs. In chapter 3.4, we demonstrated that the knockdown of NEAT1 alleviated LDs accumulation in primary microglia exposed to hypoxia. In chapter 3.5, we found that silencing NEAT1 could repress OGD/R-induced autophagy in microglia cells and demonstrated that Atg3, Atg5, and Beclin1 were involved in the process of NEAT1 restrained autophagy. Further, 3-MA and RAPA were used to inhibit/activate autophagy, in turn to illustrate the interaction of autophagy and LDs accumulation. In a normal physiological state, autophagy can phagocytose and degrade excess lipids and participate in lipid metabolism called lipophagy (macrolipophagy or microlipophagy) (Kloska et al. 2020). Under nutrient deficiency conditions, the lipid is encapsulated in a double membrane autophagosome and transported to lysosomes to be degraded into free fatty acids to provide energy for the body (Zhang S et al. 2022). This process can select the recognition and degradation of lipids, then regulate lipid metabolism in cells and maintain intracellular lipid homeostasis. Lipophagy is regulated by genes, enzymes, transcriptional regulators, and other factors. It has been shown that lipophagy and autophagy have synergistic or cross effects (Liu und Czaja 2013). For example, lipase-induced LD degradation partially depends on the autophagy pathway (Xie et al. 2020). Branched-chain amino acids have been shown to promote liver injury in obese/diabetic mice by increasing adipocytes lipolysis and suppressing heptic autophagy (Zhang F. et al. 2016). Since both cytoplasmic lipase (ATGL) and hormone-sensitive lipase can directly interact with LC3, it is speculated that lipophagy in the liver has a synergistic effect with lipolysis, and the activity of ATGL is related to lipophagy. Overexpression of ATGL will increase lipophagy in the liver through SIRT1 (Sathyanarayan et al. 2017). One study used rat primary hepatic cells cultured with oleic acid or methionine- and choline- deficient medium (MCDM) and treated with 3-MA or Atg5 siRNA to inhibit autophagy (Singh R. et al. 2009). It was found that the level of intracellular TGs increased, and the number and volume of LDs increased. At the same time, fatty acid β-oxidation decreased. The co-localization of LDs and autophagy

signaling protein LC3 showed that LDs could be observed in autophagy vesicles in cultured hepatocytes and mouse liver tissues regardless of the state of basal or enhanced autophagy. They also observed that hepatocytes cultured with oleic acid or MCDM contained more LDs within autophagic vesicles than controls (Singh R et al. 2009). In addition, in the specific Atg7 knockout mouse model, Oil red O staining showed that the LDs in the liver increased, and the levels of TGs and LD-related proteins TIP47 and ADRP also increased (Dice 1990). All these findings suggest that hepatic fat deposition increases after inhibiting autophagy, whereas autophagy appears to have the opposite effect on fat than in hepatocytes (Zhang Y et al. 2009). Normal wildtype mice fed with a high fat diet for several weeks gained weight, and white fat tissue was significantly increased. However, there were no significant changes in a targeted deletion of Atg7 in the adipose tissue of the mice both in body weight and fat content compared to normal mice. The mutant mice fed with a regular diet had significantly less white adipose tissue than wild-type mice. Thus, unlike promoting lipolysis in the liver, autophagy promotes lipid storage in adipocytes (Zhang Y et al. 2009), which coincides with the result of this study. Here, it is shown that the expression of LDs was reduced in hypoxic microglia after blocking the autophagic pathway. This result was also consistent with one study by Xu and colleagues. They knocked out the Atg7 gene in both primary microglia and BV2 cells and reported that apolipoprotein E (ApoE), a significant cholesterol and lipid transporter, was raised in these two kinds of cells. Intriguingly, higher levels of LDs were revealed in BV2 cells compared with control groups (Xu et al. 2021).

4.6. Limitations

There are some limitations of this study that need to be mentioned. First, the experiments did not explore the direct targets of NEAT1, although changes in downstream mRNA and protein levels after NEAT1 knockdown were tested using qRT-PCR and western blot. Furthermore, the results of the co-culture experiments with primary microglia and SH-SY5Y cells suggest that the knockdown of NEAT1 in microglia protects SH-SY5Y cells from OGD injury. Though, present results demonstrate that NEAT1 could regulate the autophagy, inflammation, and LDs levels in primary microglia after exposure to hypoxia. However, the exact mechanism of how NEAT1 improves SH-SY5Y cell survival rate requires further exploration. One can assume that by reducing the inflammation in SH-SY5Y cells or regulating LD metabolism NEAT1 could regulate the expression of TREM2. Furthermore, future experiments should explore in more detail which components of the

LDs are affected by NEAT1 (free fatty acids or cholesterol)? Finally, the effects of NEAT1 on LD formation and inflammation have to be verified in animal models of ischemic stroke.

5. Summary

In this project, it was investigated whether NEAT1, LDs, and autophagy-related genes were changed under hypoxia conditions in primary microglia cells in vitro. Further, the significance of NEAT1 knockdown on lipid metabolism, autophagy, and neurons in an OGD cell culture model was evaluated. First, primary microglia were isolated from newborn mice. The expression of NEAT1, LDs, and autophagy-related genes was shown to be elevated after exposure to OGD. Secondly, ASO NEAT1 was used to silence NEAT1 in primary microglia cells. After knockdown of NEAT1, the accumulation of LDs was inhibited and the expression of autophagy-related genes was also decreased. The autophagy inducer RAPA reversed the down-regulation of LD accumulation and PLIN2 expression patterns induced by ASO NEAT1 under OGD/R condition in microglia, whereas the autophagy inhibitor 3-MA promoted those effects. Finally, it was shown that the knockdown of NEAT1 protects SH-SY5Y cells from OGD injury. These findings support the hypothesis that NEAT1 may serve as a promising target for the treatment of ischemic stroke.

APPENDIX

Wenqiang X, Wei W, Yongli P, Baolong C, Xinyu Y (2021): Modulating poststroke inflammatory mechanisms: Novel aspects of mesenchymal stem cells, extracellular vesicles and microglia. World Stem Cells. 2021, 13 (8),1030-1048.

6. References

Adibhatla RM, Hatcher JF (2005): Cytidine 5'-diphosphocholine (CDP-choline) in stroke and other CNS disorders. Neurochem Res 30, 15-23

An J, Lv W, Zhang Y (2017): LncRNA NEAT1 contributes to paclitaxel resistance of ovarian cancer cells by regulating ZEB1 expression via miR-194. OncoTargets and therapy 10, 5377-5390

Anrather J, Iadecola C (2016): Inflammation and Stroke: An Overview. Neurotherapeutics : the journal of the American Society for Experimental NeuroTherapeutics 13, 661-670

Bai QK, Zhao ZG, Lu LJ, Shen J, Zhang JY, Sui HJ, Xie XH, Chen J, Yang J, Chen CR (2019): Treating ischaemic stroke with intravenous tPA beyond 4.5 hours under the guidance of a MRI DWI/T2WI mismatch was safe and effective. Stroke Vasc Neurol 4, 8-13

Balami JS, Hadley G, Sutherland BA, Karbalai H, Buchan AM (2013): The exact science of stroke thrombolysis and the quiet art of patient selection. Brain 136, 3528-3553

Bao M, Szeto V, Yang B, Zhu S, Sun H, Feng Z (2018): Long non-coding RNAs in ischemic stroke. Cell death & disease 9, 281

Barthels D, Das H (2020): Current advances in ischemic stroke research and therapies. Biochimica et biophysica acta. Molecular basis of disease 1866, 165260

Bennett M, Wasiak J, Schnabel A, Kranke P, French C (2005): Hyperbaric oxygen therapy for acute ischaemic stroke. The Cochrane database of systematic reviews, CD004954

Bhaskar S, Stanwell P, Cordato D, Attia J, Levi C (2018): Reperfusion therapy in acute ischemic stroke: dawn of a new era? BMC neurology 18, 8

Bhatia P, Kaur G, Singh N (2021): Ozagrel a thromboxane A2 synthase inhibitor extenuates endothelial dysfunction, oxidative stress and neuroinflammation in rat model of bilateral common carotid artery occlusion induced vascular dementia. Vascular pharmacology 137, 106827

Bu F, Wang A, Zhu Y, You H, Zhang Y, Meng X, Huang C, Li J (2020): LncRNA NEAT1: Shedding light on mechanisms and opportunities in liver diseases. Liver international : official journal of the International Association for the Study of the Liver 40, 2612-2626

Carloni S, Buonocore G, Balduini W (2008): Protective role of autophagy in neonatal hypoxia-ischemia induced brain injury. Neurobiology of disease 32, 329-339

Chamorro Á, Dirnagl U, Urra X, Planas A (2016): Neuroprotection in acute stroke: targeting excitotoxicity, oxidative and nitrosative stress, and inflammation. The Lancet. Neurology 15, 869-881

Chaves CJ, Caplan LR (2000): Heparin and oral anticoagulants in the treatment of brain ischemia. J Neurol Sci 173, 3-9

Chen J, Luo X, Liu M, Peng L, Zhao Z, He C, He Y (2021): Silencing long non-coding RNA NEAT1 attenuates rheumatoid arthritis via the MAPK/ERK signalling pathway by downregulating microRNA-129 and microRNA-204. RNA biology 18, 657-668

Chen W, Sun Y, Liu K, Sun X (2014): Autophagy: a double-edged sword for neuronal survival after cerebral ischemia. Neural Regen Res 9, 1210-1216

Chong J, Mohr J (2005): Anticoagulation and platelet antiaggregation therapy in stroke prevention. Current opinion in neurology 18, 53-57

Chrostek MR, Fellows EG, Crane AT, Grande AW, Low WC (2019): Efficacy of stem cell-based therapies for stroke. Brain Res 1722, 146362

Cole N, Murphy D, Grider T, Rueter S, Brasaemle D, Nussbaum R (2002): Lipid droplet binding and oligomerization properties of the Parkinson's disease protein alpha-synuclein. The Journal of biological chemistry 277, 6344-6352

Colonna M, Butovsky O (2017): Microglia Function in the Central Nervous System During Health and Neurodegeneration. Annual review of immunology 35, 441-468

Dhiman R, Caesar S, Thiam A, Schrul B (2020): Mechanisms of protein targeting to lipid droplets: A unified cell biological and biophysical perspective. Seminars in cell & developmental biology 108, 4-13

Dice J (1990): Peptide sequences that target cytosolic proteins for lysosomal proteolysis. Trends in biochemical sciences 15, 305-309

Dong LI, Zheng Y, Gao L, Luo X (2021): lncRNA NEAT1 prompts autophagy and apoptosis in MPTP-induced Parkinson's disease by impairing miR-374c-5p. Acta Biochim Biophys Sin (Shanghai) 53, 870-882

Donnan G, Fisher M, Macleod M, Davis S (2008): Stroke. Lancet (London, England) 371, 1612-1623

Drew K, Rice M, Kuhn T, Smith M (2001): Neuroprotective adaptations in hibernation: therapeutic implications for ischemia-reperfusion, traumatic brain injury and neurodegenerative diseases. Free radical biology & medicine 31, 563-573

Durukan A, Tatlisumak T (2007): Acute ischemic stroke: overview of major experimental rodent models, pathophysiology, and therapy of focal cerebral ischemia. Pharmacology, biochemistry, and behavior 87, 179-197

Edlow JA (2018): Managing Patients With Transient Ischemic Attack. Ann Emerg Med 71, 409-415

Fan G, Zhang C, Wei X, Wei R, Qi Z, Chen K, Cai X, Xu L, Tang L, Zhou J, et al. (2021): NEAT1/hsa-miR-372-3p axis participates in rapamycin-induced lipid metabolic disorder. Free radical biology & medicine 167, 1-11

Fang L, Sun J, Pan Z, Song Y, Zhong L, Zhang Y, Liu Y, Zheng X, Huang P (2017): Long non-coding RNA NEAT1 promotes hepatocellular carcinoma cell proliferation through the regulation of miR-129-5p-VCP-IκB. American journal of physiology. Gastrointestinal and liver physiology 313, G150-G156

Fitzner D, Bader J, Penkert H, Bergner C, Su M, Weil M, Surma M, Mann M, Klose C, Simons M (2020): Cell-Type- and Brain-Region-Resolved Mouse Brain Lipidome. Cell reports 32, 108132

Forreider B, Pozivilko D, Kawaji Q, Geng X, Ding Y (2017): Hibernation-like neuroprotection in stroke by attenuating brain metabolic dysfunction. Progress in neurobiology 157, 174-187

Fumagalli S, Perego C, Pischiutta F, Zanier ER, De Simoni MG (2015): The ischemic environment drives microglia and macrophage function. Front Neurol 6, 81

Gai W, Yuan H, Li X, Power J, Blumbergs P, Jensen P (2000): In situ and in vitro study of colocalization and segregation of alpha-synuclein, ubiquitin, and lipids in Lewy bodies. Experimental neurology 166, 324-333

Gao N, Li Y, Li J, Gao Z, Yang Z, Li Y, Liu H, Fan T (2020): Long Non-Coding RNAs: The Regulatory Mechanisms, Research Strategies, and Future Directions in Cancers. Frontiers in oncology 10, 598817

Gasparovic C, Rosenberg G, Wallace J, Estrada E, Roberts K, Pastuszyn A, Ahmed W, Graham G (2001): Magnetic resonance lipid signals in rat brain after experimental stroke correlate with neutral lipid accumulation. Neuroscience letters 301, 87-90

Ghafouri-Fard S, Shoorei H, Taheri M (2020): Non-coding RNAs participate in the ischemia-reperfusion injury. Biomedicine & pharmacotherapy = Biomedecine & pharmacotherapie 129, 110419

Green DR, Levine B (2014): To be or not to be? How selective autophagy and cell death govern cell fate. Cell 157, 65-75

Greenberg A, Egan J, Wek S, Garty N, Blanchette-Mackie E, Londos C (1991): Perilipin, a major hormonally regulated adipocyte-specific phosphoprotein associated with the periphery of lipid storage droplets. The Journal of biological chemistry 266, 11341-11346

Guo S, Wang H, Yin Y (2022): Microglia Polarization From M1 to M2 in Neurodegenerative Diseases. Front Aging Neurosci 14, 815347

Halladin NL (2015): Oxidative and inflammatory biomarkers of ischemia and reperfusion injuries. Dan Med J 62, B5054

Hao Y, Xin M, Feng L, Wang X, Wang X, Ma D, Feng J (2020): Review Cerebral Ischemic Tolerance and Preconditioning: Methods, Mechanisms, Clinical Applications, and Challenges. Frontiers in neurology 11, 812

Harada S, Fujita-Hamabe W, Tokuyama S (2012): Ischemic stroke and glucose intolerance: a review of the evidence and exploration of novel therapeutic targets. J Pharmacol Sci 118, 1-13

Hariri H, Rogers S, Ugrankar R, Liu Y, Feathers J, Henne W (2018): Lipid droplet biogenesis is spatially coordinated at ER-vacuole contacts under nutritional stress. EMBO reports 19, 57-72

He L, Zhang J, Zhao J, Ma N, Kim SW, Qiao S, Ma X (2018): Autophagy: The Last Defense against Cellular Nutritional Stress. Adv Nutr 9, 493-504

Hong K, Saver J (2010): Years of disability-adjusted life gained as a result of thrombolytic therapy for acute ischemic stroke. Stroke 41, 471-477

Huang H, He W, Tang T, Qiu M (2022): Immunological Markers for Central Nervous System Glia. Neuroscience bulletin

Huang H, He W, Tang T, Qiu M (2022): Immunological Markers for Central Nervous System Glia. Neurosci Bull

Huang J, Manning BD (2008): The TSC1-TSC2 complex: a molecular switchboard controlling cell growth. Biochem J 412, 179-190

Huang-Fu N, Cheng JS, Wang Y, Li ZW, Wang SH (2018): Neat1 regulates oxidized low-density lipoprotein-induced inflammation and lipid uptake in macrophages via paraspeckle formation. Mol Med Rep 17, 3092-3098

Hung CM, Garcia-Haro L, Sparks CA, Guertin DA (2012): mTOR-dependent cell survival mechanisms. Cold Spring Harb Perspect Biol 4

Iadecola C, Buckwalter M, Anrather J (2020): Immune responses to stroke: mechanisms, modulation, and therapeutic potential. The Journal of clinical investigation 130, 2777-2788

Imamura K, Imamachi N, Akizuki G, Kumakura M, Kawaguchi A, Nagata K, Kato A, Kawaguchi Y, Sato H, Yoneda M, et al. (2014): Long noncoding RNA NEAT1-dependent SFPQ relocation from promoter region to paraspeckle mediates IL8 expression upon immune stimuli. Molecular cell 53, 393-406

Jen J, Tang Y, Lu Y, Lin C, Lai W, Wang Y (2017): Oct4 transcriptionally regulates the expression of long non-coding RNAs NEAT1 and MALAT1 to promote lung cancer progression. Molecular cancer 16, 104

Ji Z, Song R, Regev A, Struhl K (2015): Many lncRNAs, 5'UTRs, and pseudogenes are translated and some are likely to express functional proteins. eLife 4, e08890

Jia H, He J, Zhao L, Hsu C, Zhao X, Du Y, Han L, Cui Z, Shi X, Ye H (2022): Combination of stem cell therapy and acupuncture to treat ischemic stroke: a prospective review. Stem cell research & therapy 13, 87

Jiang P, Mizushima N (2015): LC3- and p62-based biochemical methods for the analysis of autophagy progression in mammalian cells. Methods 75, 13-18

Jin F, Ou W, Wei B, Fan H, Wei C, Fang D, Li G, Liu W, Liu J, Jin L, et al. (2021): Neat1Transcriptome-Wide Analysis to Identify the Inflammatory Role of lncRNA in Experimental Ischemic Stroke. Journal of inflammation research 14, 2667-2680

Jin S, Lin C, Lin X, Zheng J, Guan H (2022): Silencing lncRNA NEAT1 reduces nonalcoholic fatty liver fat deposition by regulating the miR-139-5p/c-Jun/SREBP-1c pathway. Annals of hepatology 27, 100584

Jordán J, Ikuta I, García-García J, Calleja S, Segura T (2007): Stroke pathophysiology: management challenges and new treatment advances. Journal of physiology and biochemistry 63, 261-277

Jung CH, Ro SH, Cao J, Otto NM, Kim DH (2010): mTOR regulation of autophagy. FEBS Lett 584, 1287-1295

Juni R, 't Hart K, Houtkooper R, Boon R (2022): Long noncoding RNAs in cardiometabolic disorders. FEBS letters 596, 1367-1387

Karlsson O, Baccarelli A (2016): Environmental Health and Long Non-coding RNAs. Current environmental health reports 3, 178-187

Kawabori M, Shichinohe H, Kuroda S, Houkin K (2020): Clinical Trials of Stem Cell Therapy for Cerebral Ischemic Stroke. Int J Mol Sci 21

Ke H, Zhao L, Feng X, Xu H, Zou L, Yang Q, Su X, Peng L, Jiao B (2016): NEAT1 is Required for Survival of Breast Cancer Cells Through FUS and miR-548. Gene regulation and systems biology 10, 11-17

Kiphuth I, Köhrmann M, Huttner H, Schellinger P (2009): The safety and usefulness of low molecular weight heparins and unfractionated heparins in patients with acute stroke. Expert opinion on drug safety 8, 585-597

Klionsky DJ, Emr SD (2000): Autophagy as a regulated pathway of cellular degradation. Science 290, 1717-1721

Kloska A, Węsierska M, Malinowska M, Gabig-Cimińska M, Jakóbkiewicz-Banecka J (2020): Lipophagy and Lipolysis Status in Lipid Storage and Lipid Metabolism Diseases. Int J Mol Sci 21

Krafft P, Bailey E, Lekic T, Rolland W, Altay O, Tang J, Wardlaw J, Zhang J, Sudlow C (2012): Etiology of stroke and choice of models. International journal of stroke : official journal of the International Stroke Society 7, 398-406

Kreutzberg GW (1996): Microglia: a sensor for pathological events in the CNS. Trends Neurosci 19, 312-318

Kristián T (2004): Metabolic stages, mitochondria and calcium in hypoxic/ischemic brain damage. Cell calcium 36, 221-233

Kung J, Colognori D, Lee J (2013): Long noncoding RNAs: past, present, and future. Genetics 193, 651-669

Kuriakose D, Xiao Z (2020): Pathophysiology and Treatment of Stroke: Present Status and Future Perspectives. International journal of molecular sciences 21

Kwak K, Kwon H, Lee J, Park Y (2018): Current Perspectives Regarding Stem Cell-based Therapy for Ischemic Stroke. Current pharmaceutical design 24, 3332-3340

Kwak KA, Kwon HB, Lee JW, Park YS (2018): Current Perspectives Regarding Stem Cell-based Therapy for Ischemic Stroke. Curr Pharm Des 24, 3332-3340

Kwon Y, Kim J, Kim C, Tu T, Kim M, Suk K, Kim D, Lee B, Choi H, Park T, et al. (2017): Hypothalamic lipid-laden astrocytes induce microglia migration and activation. FEBS letters 591, 1742-1751

Lanzillotti C, De Mattei M, Mazziotta C, Taraballi F, Rotondo JC, Tognon M, Martini F (2021): Long Non-coding RNAs and MicroRNAs Interplay in Osteogenic Differentiation of Mesenchymal Stem Cells. Front Cell Dev Biol 9, 646032

Lee KH, Cha M, Lee BH (2021): Crosstalk between Neuron and Glial Cells in Oxidative Injury and Neuroprotection. Int J Mol Sci 22

Li P, Duan S, Fu A (2020): Long noncoding RNA NEAT1 correlates with higher disease risk, worse disease condition, decreased miR-124 and miR-125a and predicts poor recurrence-free survival of acute ischemic stroke. Journal of clinical laboratory analysis 34, e23056

Li W, Zhang Z, Liu X, Cheng X, Zhang Y, Han X, Zhang Y, Liu S, Yang J, Xu B, et al. (2017): The FOXN3-NEAT1-SIN3A repressor complex promotes progression of hormonally responsive breast cancer. The Journal of clinical investigation 127, 3421-3440

Li Y, Guo W, Cai Y (2020): NEAT1 Promotes LPS-induced Inflammatory Injury in Macrophages by Regulating MiR-17-5p/TLR4. Open medicine (Warsaw, Poland) 15, 38-49

Lian H, Roy E, Zheng H (2016): Protocol for Primary Microglial Culture Preparation. Bio Protoc 6

Lian H, Roy E, Zheng H (2016): Protocol for Primary Microglial Culture Preparation. Bio-protocol 6

Lian X, Luo B (2021): Knockdown of NEAT1 induced microglial M2 polarization via miR-374a-5p/NFAT5 axis to inhibit inflammatory response caused by OGD/R. Acta neurobiologiae experimentalis 81, 362-374

Liang J, Liu C, Xu D, Xie K, Li A (2022): LncRNA NEAT1 facilitates glioma progression via stabilizing PGK1. Journal of translational medicine 20, 80

Lin CH, Liao LY, Yang TY, Chang YJ, Tung CW, Hsu SL, Hsueh CM (2019): Microglia-Derived Adiposomes are Potential Targets for the Treatment of Ischemic Stroke. Cell Mol Neurobiol 39, 591-604

Liu B, Xu T, Meng Y (2020): lncRNA NEAT1 aggravates cerebral ischemia/reperfusion injury by sponging miR-874-3p. Journal of biological regulators and homeostatic agents 34

Liu H, Li A, Sun Z, Zhang J, Xu H (2020): Long non-coding RNA NEAT1 promotes colorectal cancer progression by regulating miR-205-5p/VEGFA axis. Human cell 33, 386-396

Liu K, Czaja MJ (2013): Regulation of lipid stores and metabolism by lipophagy. Cell Death Differ 20, 3-11

Liu X, Liang Y, Song R, Yang G, Han J, Lan Y, Pan S, Zhu M, Liu Y, Wang Y, et al. (2018): Long non-coding RNA NEAT1-modulated abnormal lipolysis via ATGL drives hepatocellular carcinoma proliferation. Molecular cancer 17, 90

Liu Y, Wang Y, Fu X, Lu Z (2018): Long non-coding RNA NEAT1 promoted ovarian cancer cells' metastasis through regulation of miR-382-3p/ROCK1 axial. Cancer science 109, 2188-2198

Ma M, Hui J, Zhang QY, Zhu Y, He Y, Liu XJ (2018): Long non-coding RNA nuclear-enriched abundant transcript 1 inhibition blunts myocardial ischemia reperfusion injury via autophagic flux arrest and apoptosis in streptozotocin-induced diabetic rats. Atherosclerosis 277, 113-122

Mariani E, Frabetti F, Tarozzi A, Pelleri M, Pizzetti F, Casadei R (2016): Meta-Analysis of Parkinson's Disease Transcriptome Data Using TRAM Software: Whole Substantia Nigra Tissue and Single Dopamine Neuron Differential Gene Expression. PloS one 11, e0161567

Marschallinger J, Iram T, Zardeneta M, Lee S, Lehallier B, Haney M, Pluvinage J, Mathur V, Hahn O, Morgens D, et al. (2020): Lipid-droplet-accumulating microglia represent a dysfunctional and proinflammatory state in the aging brain. Nature neuroscience 23, 194-208

Marschallinger J, Iram T, Zardeneta M, Lee SE, Lehallier B, Haney MS, Pluvinage JV, Mathur V, Hahn O, Morgens DW, et al. (2020): Lipid-droplet-accumulating microglia represent a dysfunctional and proinflammatory state in the aging brain. Nat Neurosci 23, 194-208

Martin EC, Rhodes LV, Elliott S, Krebs AE, Nephew KP, Flemington EK, Collins-Burow BM, Burow ME (2014): microRNA regulation of mammalian target of rapamycin expression and activity controls estrogen receptor function and RAD001 sensitivity. Mol Cancer 13, 229

Mattson MP (2008): Glutamate and neurotrophic factors in neuronal plasticity and disease. Ann N Y Acad Sci 1144, 97-112

McClendon E, Wang K, Degener-O'Brien K, Hagen M, Gong X, Nguyen T, Wu W, Maylie J, Back S (2019): Transient Hypoxemia Disrupts Anatomical and Functional Maturation of Preterm Fetal Ovine CA1 Pyramidal Neurons. The Journal of neuroscience : the official journal of the Society for Neuroscience 39, 7853-7871

Miller E, Boehme A, Chung N, Wang S, Lacey J, Lakshminarayan K, Zhong C, Woo D, Bello N, Wapner R, et al. (2019): Aspirin reduces long-term stroke risk in women with prior hypertensive disorders of pregnancy. Neurology 92, e305-e316

Mizushima N, Komatsu M (2011): Autophagy: renovation of cells and tissues. Cell 147, 728-741

Murrow L, Debnath J (2013): Autophagy as a stress-response and quality-control mechanism: implications for cell injury and human disease. Annu Rev Pathol 8, 105-137

Musuka T, Wilton S, Traboulsi M, Hill M (2015): Diagnosis and management of acute ischemic stroke: speed is critical. CMAJ : Canadian Medical Association journal = journal de l'Association medicale canadienne 187, 887-893

Muthaian R, Minhas G, Anand A (2012): Pathophysiology of stroke and stroke-induced retinal ischemia: emerging role of stem cells. Journal of cellular physiology 227, 1269-1279

Nakagawa S, Naganuma T, Shioi G, Hirose T (2011): Paraspeckles are subpopulation-specific nuclear bodies that are not essential in mice. The Journal of cell biology 193, 31-39

Ni X, Su Q, Xia W, Zhang Y, Jia K, Su Z, Li G (2020): Knockdown lncRNA NEAT1 regulates the activation of microglia and reduces AKT signaling and neuronal apoptosis after cerebral ischemic reperfusion. Scientific reports 10, 19658

o. Autor (2019): Global, regional, and national burden of stroke, 1990-2016: a systematic analysis for the Global Burden of Disease Study 2016. The Lancet. Neurology 18, 439-458

Olzmann J, Carvalho P (2019): Dynamics and functions of lipid droplets. Nature reviews. Molecular cell biology 20, 137-155

Ortega M, Fraile-Martinez O, García-Montero C, Callejón-Peláez E, Sáez M, Álvarez-Mon M, García-Honduvilla N, Monserrat J, Álvarez-Mon M, Bujan J, et al. (2021): A General Overview on the Hyperbaric Oxygen Therapy: Applications, Mechanisms and Translational Opportunities. Medicina (Kaunas, Lithuania) 57

Pan S, Liu R, Wu X, Ma K, Luo W, Nie K, Zhang C, Meng X, Tong T, Chen X, et al. (2021): LncRNA NEAT1 mediates intestinal inflammation by regulating TNFRSF1B. Ann Transl Med 9, 773

Panuganti KK, Tadi P, Lui F: Transient Ischemic Attack. StatPearls. StatPearls Publishing

Copyright © 2022, StatPearls Publishing LLC., Treasure Island (FL) 2022

Peng L, Hu G, Yao Q, Wu J, He Z, Law BY, Hu G, Zhou X, Du J, Wu A, et al. (2022): Microglia autophagy in ischemic stroke: A double-edged sword. Front Immunol 13, 1013311

Perry VH, Teeling J (2013): Microglia and macrophages of the central nervous system: the contribution of microglia priming and systemic inflammation to chronic neurodegeneration. Semin Immunopathol 35, 601-612

Pham-Huy L, He H, Pham-Huy C (2008): Free radicals, antioxidants in disease and health. International journal of biomedical science : IJBS 4, 89-96

Prabhakaran S, Ruff I, Bernstein RA (2015): Acute stroke intervention: a systematic review. Jama 313, 1451-1462

Präbst K, Engelhardt H, Ringgeler S, Hübner H (2017): Basic Colorimetric Proliferation Assays: MTT, WST, and Resazurin. Methods Mol Biol 1601, 1-17

Prinz F, Kapeller A, Pichler M, Klec C (2019): The Implications of the Long Non-Coding RNA NEAT1 in Non-Cancerous Diseases. Int J Mol Sci 20

Qin C, Zhou LQ, Ma XT, Hu ZW, Yang S, Chen M, Bosco DB, Wu LJ, Tian DS (2019): Dual Functions of Microglia in Ischemic Stroke. Neurosci Bull 35, 921-933

Qin C, Yang S, Chu YH, Zhang H, Pang XW, Chen L, Zhou LQ, Chen M, Tian DS, Wang W (2022): Signaling pathways involved in ischemic stroke: molecular mechanisms and therapeutic interventions. Signal Transduct Target Ther 7, 215

Rabinowitz JD, White E (2010): Autophagy and metabolism. Science 330, 1344-1348

Ralhan I, Chang C, Lippincott-Schwartz J, Ioannou M (2021): Lipid droplets in the nervous system. The Journal of cell biology 220

Ryter SW, Cloonan SM, Choi AM (2013): Autophagy: a critical regulator of cellular metabolism and homeostasis. Mol Cells 36, 7-16

Sandercock P, Leong T (2017): Low-molecular-weight heparins or heparinoids versus standard unfractionated heparin for acute ischaemic stroke. The Cochrane database of systematic reviews 4, CD000119

Sandercock P, Counsell C, Tseng M (2008): Low-molecular-weight heparins or heparinoids versus standard unfractionated heparin for acute ischaemic stroke. The Cochrane database of systematic reviews, CD000119

Sandercock P, Counsell C, Tseng M, Cecconi E (2014): Oral antiplatelet therapy for acute ischaemic stroke. The Cochrane database of systematic reviews, CD000029

Santoro M, Nociti V, Lucchini M, De Fino C, Losavio F, Mirabella M (2016): Expression Profile of Long Non-Coding RNAs in Serum of Patients with Multiple Sclerosis. Journal of molecular neuroscience : MN 59, 18-23

Sarkar S (2013): Regulation of autophagy by mTOR-dependent and mTOR-independent pathways: autophagy dysfunction in neurodegenerative diseases and therapeutic application of autophagy enhancers. Biochem Soc Trans 41, 1103-1130

Sathyanarayan A, Mashek MT, Mashek DG (2017): ATGL Promotes Autophagy/Lipophagy via SIRT1 to Control Hepatic Lipid Droplet Catabolism. Cell Rep 19, 1-9

Shen S, Ma L, Shao F, Jin L, Bian Z (2020): Long Non-Coding RNA (lncRNA) NEAT1 Aggravates Cerebral Ischemia-Reperfusion Injury by Suppressing the Inhibitory Effect of miR-214 on PTEN. Medical science monitor : international medical journal of experimental and clinical research 26, e924781

Shen Z, Xiang M, Chen C, Ding F, Wang Y, Shang C, Xin L, Zhang Y, Cui X (2022): Glutamate excitotoxicity: Potential therapeutic target for ischemic stroke. Biomedicine & pharmacotherapy = Biomedecine & pharmacotherapie 151, 113125

Shimabukuro M, Langhi L, Cordeiro I, Brito J, Batista C, Mattson M, Mello Coelho V (2016): Lipid-laden cells differentially distributed in the aging brain are functionally active and correspond to distinct phenotypes. Scientific reports 6, 23795

Singh B, Bhaskar S (2019): Methods for Detection of Autophagy in Mammalian Cells. Methods Mol Biol 2045, 245-258

Singh R, Kaushik S, Wang Y, Xiang Y, Novak I, Komatsu M, Tanaka K, Cuervo A, Czaja M (2009): Autophagy regulates lipid metabolism. Nature 458, 1131-1135

Singh R, Kaushik S, Wang Y, Xiang Y, Novak I, Komatsu M, Tanaka K, Cuervo AM, Czaja MJ (2009): Autophagy regulates lipid metabolism. Nature 458, 1131-1135

Soayfane Z, Tercé F, Cantiello M, Robenek H, Nauze M, Bézirard V, Allart S, Payré B, Capilla F, Cartier C, et al. (2016): Exposure to dietary lipid leads to rapid production of cytosolic lipid droplets near the brush border membrane. Nutrition & metabolism 13, 48

Stadelmann C, Timmler S, Barrantes-Freer A, Simons M (2019): Myelin in the Central Nervous System: Structure, Function, and Pathology. Physiol Rev 99, 1381-1431

Statello L, Guo C, Chen L, Huarte M (2021): Author Correction: Gene regulation by long non-coding RNAs and its biological functions. Nature reviews. Molecular cell biology 22, 159

Sun F, Liu H, Fu H, Zhang S, Qian X, Li J, Zhu Y, Zhang X, Zhang J, Qiu H, et al. (2020): Comparative study of intravenous thrombolysis with rt-PA and urokinase for patients with acute cerebral infarction. The Journal of international medical research 48, 300060519895352

Sun M, Jin H, Sun X, Huang S, Zhang F, Guo Z, Yang Y (2018): Free Radical Damage in Ischemia-Reperfusion Injury: An Obstacle in Acute Ischemic Stroke after Revascularization Therapy. Oxidative medicine and cellular longevity 2018, 3804979

Taguchi A, Soma T, Tanaka H, Kanda T, Nishimura H, Yoshikawa H, Tsukamoto Y, Iso H, Fujimori Y, Stern D, et al. (2004): Administration of CD34+ cells after stroke enhances neurogenesis via angiogenesis in a mouse model. The Journal of clinical investigation 114, 330-338

Tanida I, Ueno T, Kominami E (2004): LC3 conjugation system in mammalian autophagy. Int J Biochem Cell Biol 36, 2503-2518

Tao Q, Tianyu W, Jiangqiao Z, Zhongbao C, Xiaoxiong M, Long Z, Jilin Z (2019): Expression analysis of long non-coding RNAs in a renal ischemia-reperfusion injury model. Acta cirurgica brasileira 34, e201900403

Thiankhaw K, Chattipakorn N, Chattipakorn S (2021): The effects of hyperbaric oxygen therapy on the brain with middle cerebral artery occlusion. Journal of cellular physiology 236, 1677-1694

Veltkamp R, Warner D, Domoki F, Brinkhous A, Toole J, Busija D (2000): Hyperbaric oxygen decreases infarct size and behavioral deficit after transient focal cerebral ischemia in rats. Brain research 853, 68-73

Veltkamp R, Siebing D, Sun L, Heiland S, Bieber K, Marti H, Nagel S, Schwab S, Schwaninger M (2005): Hyperbaric oxygen reduces blood-brain barrier damage and edema after transient focal cerebral ischemia. Stroke 36, 1679-1683

Veltkamp R, Sun L, Herrmann O, Wolferts G, Hagmann S, Siebing D, Marti H, Veltkamp C, Schwaninger M (2006): Oxygen therapy in permanent brain ischemia: potential and limitations. Brain research 1107, 185-191

Venø S, Schmidt E, Bork C (2019): Polyunsaturated Fatty Acids and Risk of Ischemic Stroke. Nutrients 11

Verma M, Lizama B, Chu C (2022): Excitotoxicity, calcium and mitochondria: a triad in synaptic neurodegeneration. Translational neurodegeneration 11, 3

Vlachogiannis N, Sachse M, Georgiopoulos G, Zormpas E, Bampatsias D, Delialis D, Bonini F, Galyfos G, Sigala F, Stamatelopoulos K, et al. (2021): Adenosine-to-inosine Alu RNA editing controls the stability of the pro-inflammatory long noncoding RNA NEAT1 in atherosclerotic cardiovascular disease. Journal of molecular and cellular cardiology 160, 111-120

Walther T, Farese R (2012): Lipid droplets and cellular lipid metabolism. Annual review of biochemistry 81, 687-714

Wang C, Yang Y, Cong L, Jiang Y, Du N, Zhang H (2021): Implication of long non-coding RNA NEAT1 in the pathogenesis of bacterial meningitis-induced blood-brain barrier damage. Microvasc Res 138, 104225

Wang J, Xing H, Wan L, Jiang X, Wang C, Wu Y (2018): Treatment targets for M2 microglia polarization in ischemic stroke. Biomed Pharmacother 105, 518-525

Wang L, Xia J, Ke Z, Zhang B (2019): Blockade of NEAT1 represses inflammation response and lipid uptake via modulating miR-342-3p in human macrophages THP-1 cells. Journal of cellular physiology 234, 5319-5326

Wang P, Shao BZ, Deng Z, Chen S, Yue Z, Miao CY (2018): Autophagy in ischemic stroke. Prog Neurobiol 163-164, 98-117

Wang Q, Chen Y, Meng L, Yin J, Wang L, Gong T (2022): A Novel Perspective on Ischemic Stroke: A Review of Exosome and Noncoding RNA Studies. Brain Sci 12

Wang R, Xue S, Liu Y, Peng M, Guo B (2021): The correlation of long non-coding RNA NEAT1 and its targets microRNA (miR)-21, miR-124, and miR-125a with disease risk, severity, and inflammation of allergic rhinitis. Medicine 100, e22946

Wang S, Liu Z, Shi Z (2018): Non-Coding RNA in Acute Ischemic Stroke: Mechanisms, Biomarkers and Therapeutic Targets. Cell transplantation 27, 1763-1777

Wang Y, Hu S, Wang M, Yao R, Wu D, Yang L, Chen L (2018): Genome-wide screening of NEAT1 regulators reveals cross-regulation between paraspeckles and mitochondria. Nature cell biology 20, 1145-1158

Wang Z, Zhang S, Li K (2022): LncRNA NEAT1 induces autophagy through epigenetic regulation of autophagy-related gene expression in neuroglial cells. J Cell Physiol 237, 824-832

Wang Z, Zou Q, Song M, Chen J (2017): NEAT1 promotes cell proliferation and invasion in hepatocellular carcinoma by negative regulating miR-613 expression. Biomedicine & pharmacotherapy = Biomedecine & pharmacotherapie 94, 612-618

Wang Z, Zhao Y, Xu N, Zhang S, Wang S, Mao Y, Zhu Y, Li B, Jiang Y, Tan Y, et al. (2019): NEAT1 regulates neuroglial cell mediating Abeta clearance via the epigenetic regulation of endocytosis-related genes expression. Cell Mol Life Sci 76, 3005-3018

Watts ME, Pocock R, Claudianos C (2018): Brain Energy and Oxygen Metabolism: Emerging Role in Normal Function and Disease. Front Mol Neurosci 11, 216

Wendimu MY, Hooks SB (2022): Microglia Phenotypes in Aging and Neurodegenerative Diseases. Cells 11

Woodburn S, Bollinger J, Wohleb E (2021): The semantics of microglia activation: neuroinflammation, homeostasis, and stress. Journal of neuroinflammation 18, 258

Woolf Z, Stevenson TJ, Lee K, Jung Y, Park TIH, Curtis MA, Montgomery JM, Dragunow M (2021): Isolation of adult mouse microglia using their in vitro adherent properties. STAR Protoc 2, 100518

Wu F, Mo Q, Wan X, Dan J, Hu H (2019): NEAT1/hsa-mir-98-5p/MAPK6 axis is involved in non-small-cell lung cancer development. Journal of cellular biochemistry 120, 2836-2846

Wu M, Gu X, Ma Z (2021): Mitochondrial Quality Control in Cerebral Ischemia-Reperfusion Injury. Mol Neurobiol 58, 5253-5271

Xie Y, Li J, Kang R, Tang D (2020): Interplay Between Lipid Metabolism and Autophagy. Front Cell Dev Biol 8, 431

Xin W, Wei W, Pan Y, Cui B, Yang X, Bähr M, Doeppner T (2021): Modulating poststroke inflammatory mechanisms: Novel aspects of mesenchymal stem cells, extracellular vesicles and microglia. World journal of stem cells 13, 1030-1048

Xu Y, Shen J, Ran Z (2020): Emerging views of mitophagy in immunity and autoimmune diseases. Autophagy 16, 3-17

Xu Y, Propson NE, Du S, Xiong W, Zheng H (2021): Autophagy deficiency modulates microglial lipid homeostasis and aggravates tau pathology and spreading. Proc Natl Acad Sci U S A 118

Yan W, Chen ZY, Chen JQ, Chen HM (2018): LncRNA NEAT1 promotes autophagy in MPTP-induced Parkinson's disease through stabilizing PINK1 protein. Biochem Biophys Res Commun 496, 1019-1024

Yang J, Vitery M, Chen J, Osei-Owusu J, Chu J, Qiu Z (2019): Glutamate-Releasing SWELL1 Channel in Astrocytes Modulates Synaptic Transmission and Promotes Brain Damage in Stroke. Neuron 102, 813-827.e816

Yang Z, Zhang N, Shen H, Lin C, Lin L, Yuan B (2014): Microglial activation with reduction in autophagy limits white matter lesions and improves cognitive defects during cerebral hypoperfusion. Current neurovascular research 11, 223-229

Yarygin K, Namestnikova D, Sukhinich K, Gubskiy I, Majouga A, Kholodenko I (2021): Cell Therapy of Stroke: Do the Intra-Arterially Transplanted Mesenchymal Stem Cells Cross the Blood-Brain Barrier? Cells 10

Yeung J, Li W, Holinstat M (2018): Platelet Signaling and Disease: Targeted Therapy for Thrombosis and Other Related Diseases. Pharmacological reviews 70, 526-548

Yu Q, He Z, Zubkov D, Huang S, Kurochkin I, Yang X, Halene T, Willmitzer L, Giavalisco P, Akbarian S, et al. (2020): Lipidome alterations in human prefrontal cortex during development, aging, and cognitive disorders. Mol Psychiatry 25, 2952-2969

Zeng Y, Zhang W, Xue T, Zhang D, Lv M, Jiang Y (2022): Sphk1-induced autophagy in microglia promotes neuronal injury following cerebral ischaemia-reperfusion. The European journal of neuroscience 56, 4287-4303

Zhang F, Wu L, Qian J, Qu B, Xia S, La T, Wu Y, Ma J, Zeng J, Guo Q, et al. (2016): Identification of the long noncoding RNA NEAT1 as a novel inflammatory regulator acting through MAPK pathway in human lupus. Journal of autoimmunity 75, 96-104

Zhang F, Zhao S, Yan W, Xia Y, Chen X, Wang W, Zhang J, Gao C, Peng C, Yan F, et al. (2016): Branched Chain Amino Acids Cause Liver Injury in Obese/Diabetic Mice by Promoting Adipocyte Lipolysis and Inhibiting Hepatic Autophagy. EBioMedicine 13, 157-167

Zhang H, Liu X, Yang F, Cheng D, Liu W (2020): Overexpression of HIF-1α protects PC12 cells against OGD/R-evoked injury by reducing miR-134 expression. Cell cycle (Georgetown, Tex.) 19, 990-999

Zhang J, Yang J, Chang X, Zhang C, Zhou H, Liu M (2012): Ozagrel for acute ischemic stroke: a meta-analysis of data from randomized controlled trials. Neurological research 34, 346-353

Zhang J, Li Y, Liu Y, Xu G, Hei Y, Lu X, Liu W (2021): Long non-coding RNA NEAT1 regulates glioma cell proliferation and apoptosis by competitively binding to microRNA-324-5p and upregulating KCTD20 expression. Oncology reports 46

Zhang L, Wei W, Ai X, Kilic E, Hermann DM, Venkataramani V, Bähr M, Doeppner TR (2021): Extracellular vesicles from hypoxia-preconditioned microglia promote angiogenesis and repress apoptosis in stroke mice via the TGF-β/Smad2/3 pathway. Cell Death Dis 12, 1068

Zhang P, Cao L, Zhou R, Yang X, Wu M (2019): The lncRNA Neat1 promotes activation of inflammasomes in macrophages. Nature communications 10, 1495

Zhang S, Peng X, Yang S, Li X, Huang M, Wei S, Liu J, He G, Zheng H, Yang L, et al. (2022): The regulation, function, and role of lipophagy, a form of selective autophagy, in metabolic disorders. Cell Death Dis 13, 132

Zhang Y, Goldman S, Baerga R, Zhao Y, Komatsu M, Jin S (2009): Adipose-specific deletion of autophagy-related gene 7 (atg7) in mice reveals a role in adipogenesis. Proc Natl Acad Sci U S A 106, 19860-19865

Zhang Z, Yue P, Lu T, Wang Y, Wei Y, Wei X (2021): Role of lysosomes in physiological activities, diseases, and therapy. J Hematol Oncol 14, 79

Zhong F, Zhang W, Cao Y, Wen Q, Cao Y, Lou B, Li J, Shi W, Liu Y, Luo R, et al. (2018): LncRNA NEAT1 promotes colorectal cancer cell proliferation and migration via regulating glial cell-derived neurotrophic factor by sponging miR-196a-5p. Acta biochimica et biophysica Sinica 50, 1190-1199

Zhou Z, Lu J, Liu W, Manaenko A, Hou X, Mei Q, Huang J, Tang J, Zhang J, Yao H, et al. (2018): Advances in stroke pharmacology. Pharmacology & therapeutics 191, 23-42

Zhu J, Wan Y, Xu H, Wu Y, Hu B, Jin H (2019): The role of endogenous tissue-type plasminogen activator in neuronal survival after ischemic stroke: friend or foe? Cell Mol Life Sci 76, 1489-1506

FUNDING RELATED TO THIS THESIS

This study was supported by a scholarship from the China Scholarship Council [No. 202108080076].

ACKNOWLEDGEMENTS

Time flies and three years of a doctoral career are fleeting. At this moment, I gradually realize that studying for a doctorate is not only a learning experience but also a life experience and cognitive sublimation. Pursuing a doctorate is the continuous improvement of professional knowledge and the constant sharpening of heart and perseverance. During the three years of doctoral study, I received much help and encouragement from my professors, colleagues, and family members.

Firstly, I would like to express my sincere thanks to my supervisor Professor Thorsten R. Döppner, for his careful guidance and cultivation during my studies here. Under your careful cultivation and strict requirements, I grew step by step. From the project selection, proposal, and experiment to paper writing, every suggestion from you made me feel clear deep inside my head, every encouragement made me feel more confident, and every concern made me warm and touched. Your keen insight, rigorous scientific research thinking, excellent scientific research attitude, strong ability to condense words and simple and approachable personality charm will always be the direction of my future efforts!

I would like to thank Dr. Lars Tatenhorst and Irina Graf, who gave me careful guidance at the beginning of the design of my doctoral project and gave me great help in the process of my project and always had time for my questions.

I sincerely thank my colleagues, Wenqiang Xin and Wei Wei, who helped me with my studies and life here. Whenever I needed help, you were always there. I feel less lonely with your company in the lab for my whole doctoral career.

Finally, I sincerely thank my parents and brother for their understanding, support, and encouragement during my doctoral study. I would like to thank my parents for their hard work for our family, which is the motivation for my study and will enable me to graduate smoothly.